OSU-03012 Stimulates PKR-Like Endoplasmic Reticulum-Dependent Increases in 70-kDa Heat Shock Protein Expression, Attenuating Its Lethal Actions in Transformed Cells

Margaret A. Park, Adly Yacoub, Mohammed Rahmani, Guo Zhang, Lori Hart, Michael P. Hagan, Stuart K. Calderwood, Michael Y. Sherman, Costas Koumenis, Sarah Spiegel, Ching-Shih Chen, Martin Graf, David T. Curiel, Paul B. Fisher, Steven Grant, and Paul Dent

Departments of Biochemistry (M.A.P., A.Y., M.R., G.Z., S.S., S.G., P.D.), Medicine (M.R., S.G.), Neurosurgery (M.G.), and Radiation Oncology (A.Y.), Virginia Commonwealth University, Richmond, Virginia; Division of Medicinal Chemistry, College of Pharmacy, the Ohio State University, Columbus, Ohio (C.-S.C.); Departments of Radiation Oncology (C.K.) and Hematology/ Oncology (L.H.), University of Pennsylvania School of Medicine, Philadelphia, Pennsylvania; Department of Radiation Oncology, Harvard University, Boston, Massachusetts (S.K.C.); Departments of Pathology, Neurosurgery and Urology, Herbert Irving Comprehensive Cancer Center, Columbia University Medical Center, College of Physicians and Surgeons, New York, New York (P.B.F.); Division of Human Gene Therapy, Departments of Medicine, Pathology, and Surgery and the Gene Therapy Center, University of Alabama at Birmingham, Birmingham, Alabama (D.T.C.); and Department of Biochemistry, Boston University School of Medicine, Boston, Massachusetts (M.Y.S.)

Received October 15, 2007; accepted December 20, 2007

ABSTRACT

We have further defined mechanism(s) by which 2-amino-N-{4-[5-(2-phenanthrenyl)-3-(trifluoromethyl)-1H-pyrazol-1-yl]-phenyl}acetamide [OSU-03012 (OSU)], a derivative of the cyclooxygenase-2 (COX2) inhibitor celecoxib but lacking COX2 inhibitory activity, kills transformed cells. In cells lacking expression of protein kinase R-like endoplasmic reticulum kinase (PERK$^{-/-}$), the lethality of OSU was attenuated. OSU enhanced the expression of Beclin 1 and ATG5 and cleavage of pro-caspase 4 in a PERK-dependent fashion and promoted the Beclin 1- and ATG5-dependent formation of vacuoles containing LC3, followed by a subsequent caspase 4-dependent cleavage of cathepsin B and a cathepsin B-dependent formation of low pH intracellular vesicles; cathepsin B was activated and released into the cytosol and genetic suppression of caspase 4, cathepsin B, or apoptosis-inducing factor function significantly suppressed cell killing. In parallel, OSU caused PERK-dependent increases in 70-kDa heat shock protein (HSP70) expression and decreases in 90-kDa heat shock protein (HSP90) and Grp78/BiP expression. Changes in HSP70 expression were post-transcriptional. Knock-down or small-molecule inhibition of HSP70 expression enhanced OSU toxicity, and overexpression of HSP70 suppressed OSU-induced low pH vesicle formation and lethality. Our data demonstrate that OSU-03012 causes cell killing that is dependent on PERK-induced activation of multiple toxic proteases. OSU-03012 also increased expression of HSP70 in a PERK-dependent fashion, providing support for the contention that OSU-03012-induced PERK signaling promotes both cell survival and cell death processes.

Inhibitors of cyclooxygenase 2 (COX2) were originally developed to inhibit inflammatory immune responses, with a primary intention to use such agents clinically in the treatment of chronic diseases (e.g., rheumatoid arthritis) (Kiefer and Dannhardt, 2004; Hawkey and Fortun, 2005). It was also noted that COX2 was over-expressed in many tumor cells and that agents that inhibited COX2 [e.g., celecoxib (Cele-

ABBREVIATIONS: COX2, cyclooxygenase 2; OSU, OSU-03012 [2-amino-N-{4-[5-(2-phenanthrenyl)-3-(trifluoromethyl)-1H-pyrazol-1-yl]-phenyl}-acetamide]; ER, endoplasmic reticulum; zVAD, N-benzyloxycarbonyl-Val-Ala-Asp; AIF, apoptosis-inducing factor; PDK-1, pyruvate dehydrogenase kinase, isozyme 1; PI3K, phosphatidylinositol 3-kinase; AKT, protein kinase B; ERK1/2, extracellular signal-regulated kinase 1/2; PERK, PKR-like endoplasmic reticulum kinase; HSP70, 70-kDa heat shock protein; HSP90, 90-kDa heat shock protein; eIF2α, eukaryotic initiation factor-2α; HRP, horseradish peroxidase; GFP, green fluorescent protein; DMSO, dimethyl sulfoxide; SDS, sodium dodecyl sulfate; PAGE, polyacrylamide gel electrophoresis; 3MA, 3 methyl adenine; CMV, cytomegalovirus; siRNA, small-interfering RNA; CDTA, trans-1,2-diaminocyclohexane-N,N,N′,N′-tetra-acetic acid; MEF, mouse embryonic fibroblasts; GBM, glioblastoma multiforme; 17AAG, 17-(allylamino)-17-demethoxygeldanamycin; FITC, fluorescein isothiocyanate; SV40, simian virus 40; WT, wild type.

brex)] could suppress tumor cell growth in vitro and when grown as xenografts in animals (Koehne and Dubois, 2004; Cui et al., 2005; Kang et al., 2006; Klenke et al., 2006). Studies in patients demonstrated that persons with prolonged exposure to COX2 inhibitors as part of an anti-inflammatory therapeutic regimen also had a lower incidence of developing cancer, suggesting that COX2 inhibitors prevented cancer (Kashfi and Rigas, 2005; Narayanan et al., 2006). However, as the sensitivity of tumor cells to COX2 inhibitors was investigated in detail, it became apparent that expression of COX2 did not per se correlate with tumor cell sensitivity to COX2 inhibitor treatment (Kulp et al., 2004; Patel et al., 2005). The agent OSU-03012 was developed as an anticancer agent, with celecoxib as the chemical backbone (Zhu et al., 2004). In vitro OSU-03012 has antitumor activity an order of magnitude greater than that of celecoxib, but lacks COX2 inhibitory activity. Based on these preliminary observations, OSU-03012 was approved for development by the National Cancer Institute RAID program, with likely initiation of a phase I drug trial in 2008. Studies by our laboratory recently argued that OSU-03012 caused cell death through mechanisms that involved a form of endoplasmic reticulum (ER) stress signaling and mitochondrial dysfunction but that were a caspase-independent form of cell death, as initially judged by a lack of effect of the caspase inhibitor zVAD and expression of dominant-negative caspase 9. Instead, our findings argued that in HCT116 cells that knockdown of apoptosis-inducing factor (AIF) expression significantly attenuated OSU-03012 lethality (Yacoub et al., 2006).

In the last 5 to 10 years, multiple growth factor receptors and downstream signal transduction pathways have been linked to the advantage of tumor cells over nontransformed cells in terms of increased rates of proliferation and cell survival after exposure to toxic stresses (reviewed in Dent et al., 2003; Valerie et al., 2007). The toxicity of OSU-03012 in tumor cells was initially believed to be due to inhibition of the enzyme PDK-1, part of the PI3K pathway, inasmuch as OSU-03012 can suppress AKT phosphorylation and showed measurable inhibition of PDK-1 activity in the 5 to 50 μM range in vitro (Dent et al., 2003). OSU-03012 has also been shown to interact in a synergistic fashion with BCR-ABL inhibitors and with the ERBB2 inhibitor Herceptin to suppress tumor cell viability and to kill in a manner that is, in many cell types, at least partially caspase-independent (Johnson et al., 2005; Tseng et al., 2005; Tseng et al., 2006; To et al., 2007). In our previous studies, we also noted that inhibition of either mitogen-activated ERK1/2 or PI3K enhanced the toxicity of OSU-03012 in glioma, colon cancer, and transformed rodent fibroblast cell types (Yacoub et al., 2006). However, although OSU-03012 has been noted to suppress PDK-1 function and AKT activity, other data have also provided strong support for the contention that OSU-03012 toxicity, and its radiosensitizing effects, could not have contributed to suppression of AKT signaling (Carón et al., 2005; Yacoub et al., 2006).

In the present studies, we have again used established and primary human glioma cell lines, established colon cancer cell lines, and transformed fibroblasts lacking expression of pro-apoptotic proteins; we have examined the impact of OSU-03012 on cell viability and further defined the molecular mechanisms by which OSU-03012 enhances tumor cell death (Yacoub et al., 2006).

Materials and Methods

Materials

Phospho-/total- (extracellular signal-regulated kinase 1/2; c-Jun NH$_2$-terminal kinase 1/2; p38 mitogen-activated protein kinase) antibodies, phospho-/total-AKT (Thr308; Ser473) and the total and cleaved caspase 3 antibodies were purchased from Cell Signaling Technologies (Danvers, MA). Anti–PKR-like endoplasmic reticulum (PERK), anti-BID, anti-caspase 2, anti-caspase 4, anti-cathepsin B, pan-anti-HSP70, anti-HSP90, anti-eIF2α, and anti-eIF2α S51 antibodies were purchased from Cell Signaling Technologies. All the secondary antibodies (anti-rabbit HRP, anti-mouse HRP, and anti-goat HRP) were purchased from Santa Cruz Biotechnology (Santa Cruz, CA). Enhanced chemiluminescence (ECL) and terminal deoxynucleotidyl transferase dUTP nick-end labeling kits were purchased from PerkinElmer Life and Analytical Sciences (Waltham, MA) and Roche (Mannheim, Germany), respectively. Trypsin-EDTA, Dulbecco's modified Eagle's medium, RPMI 1640 medium, and penicillin-streptomycin were purchased from Invitrogen (Carlsbad, CA). HCT116 and U251 cells were purchased from the American Type Culture Collection (Manassas, VA). BID$^{-/-}$ fibroblasts were kindly provided by Dr. S. Korsmeyer (Harvard Medical School, Boston, MA). Transformed PERK$^{-/-}$ cells were a kind gift from the Ron Laboratory, Skirball Institute, NYU School of Medicine (New York, NY). Immortalized cathepsin B$^{-/-}$ fibroblasts and matched wild type fibroblasts were kindly supplied by Christoph Peters, Thomas Reinheckel (Medizinische Universitaetsklinik Freiburg, Freiburg, Germany) and Paul Saftig (Christian-Albrechts-Universitaet Kiel, Kiel, Germany). Short hairpin RNA plasmid constructs targeting ATG5 (pLVTHM/Atg5; a generous gift from Dr. S. Yousefi, Department of Pharmacology, University of Bern, Bern Switzerland) and Beclin-1 (pSRP-Beclin 1; kindly provided by Dr. J. Yuan, Department of Cell Biology, Harvard Medical School, Boston, MA) (Levine et al., 2005; Yang et al., 2005; Shibata et al., 2006; Yousefi et al., 2006). The level of knockdown of these autophag- related proteins in the tumor cells was determined by Western blotting with anti-ATG5 and anti-Beclin-1 antibodies (both from Santa Cruz Biotechnology). Commercially available validated short hairpin RNA molecules to knock down RNA/protein levels were from QIAGEN (Valencia, CA): ATG5, Beclin 1, AIF, caspase 4, and HSP70A/B. Primary human GBM cells and information on the genetic background of such cells were very kindly supplied for our use by Dr. C. David James (University of California, San Francisco, CA). The plasmids to express GFP-tagged human LC3, (his)$_6$ tagged hamster Grp78/BiP, dominant-negative PERK (Myc-tagged PERKΔC), and human HSP70 promoter linked to luciferase were kindly provided by Dr. S. Spiegel (Virginia Commonwealth University, Richmond, VA), Dr. A. S. Lee (USC/Norris Cancer Center, Los Angeles, CA), Dr. J. A. Diehl (University of Pennsylvania, Philadelphia, PA), and by author S.K.C., respectively. Other reagents and techniques were as described by McKinstry et al. (2002), Fehrenbacher et al. (2004); Carón et al. (2005), and Yacoub et al. (2004, 2006).

Culture and in Vitro Exposure of Cells to Drugs

All established cell lines were cultured at 37°C [5% (v/v) CO$_2$] in vitro using RPMI 1640 medium supplemented with 5% (v/v) fetal calf serum and 10% (v/v) nonessential amino acids. Primary human glioma cells were cultured in 2% (v/v) fetal calf serum to prevent growth of contaminating rodent fibroblasts during in vitro analyses. For short-term cell killing assays, immunoblotting, and AIF/cathepsin release studies, cells were plated at a density of 3×10^3 per cm^2 ($\sim 2 \times 10^5$ cells per well of a 12-well plate) and, 48 h after plating, were treated with various drugs. In vitro OSU-03012 treatment was from a 100 mM stock solution of each drug, and the maximal concentration of vehicle (DMSO) in media was 0.02% (v/v). Cells were not cultured in reduced serum media during any study reported in this article.
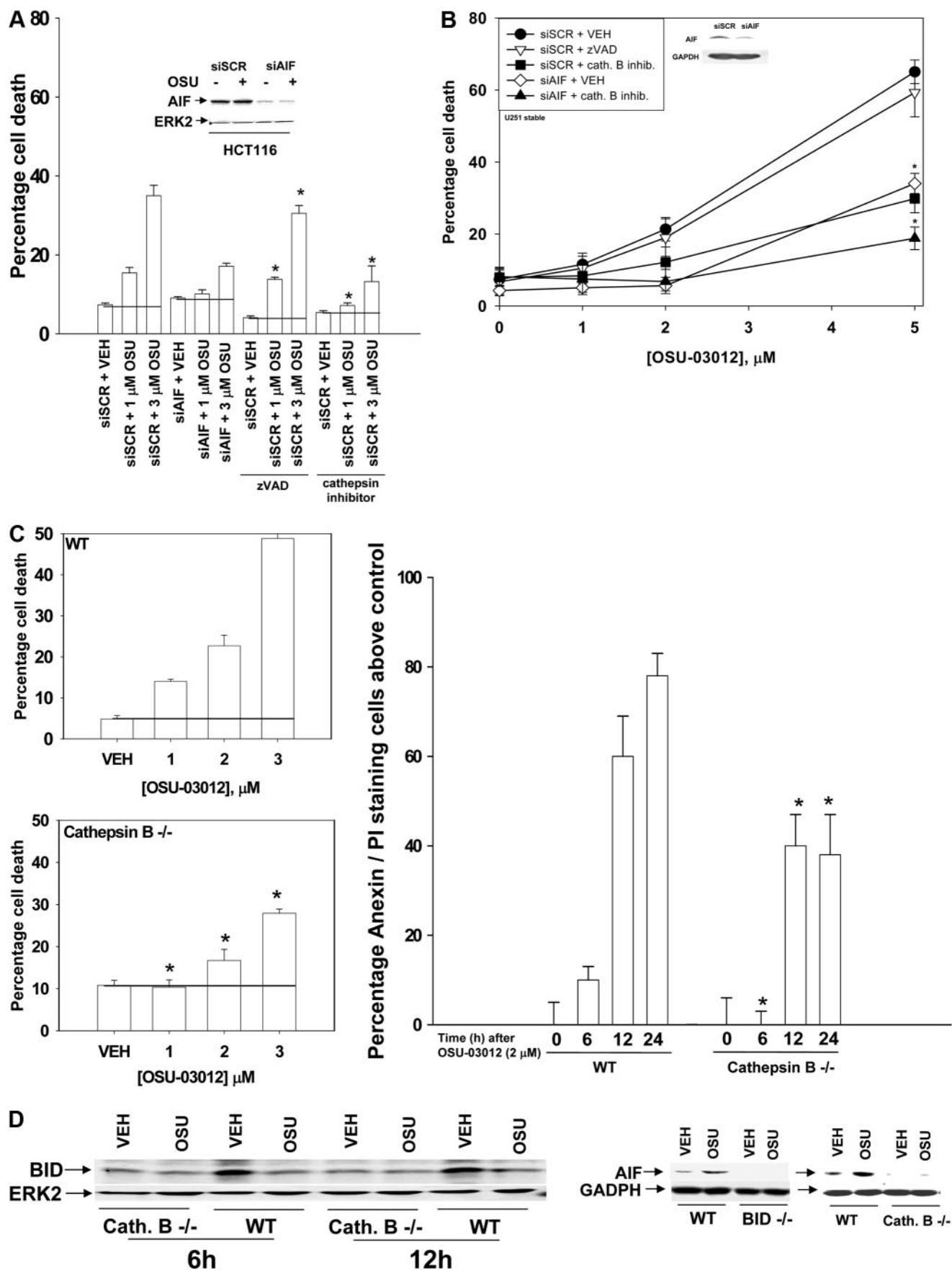
In Vitro Cell Treatments, Microscopy, SDS-PAGE, and Western Blot Analysis

For in vitro analyses of short-term cell death effects, cells were treated with vehicle or OSU-03012 for the times indicated in the figure legends. For apoptosis assays, cells were pretreated with vehicle (VEH, DMSO), zVAD (50 μM), calpain inhibitor [acetyl-Calpastatin (amino acids 184–210)] (5 μM) or cathepsin B inhibitor ([L-3-*trans*-(propylcarbamoyl)oxirane-2-carbonyl]-L-isoleucyl-L-proline methyl ester) (1 μM). Cells were isolated and either subjected to trypan blue cell viability assay by counting in a light microscope or fixed to slides and stained using a commercially available Diff Quick (Giemsa) assay kit (Yacoub et al., 2004, 2006; Carón et al., 2005). OSU-03012 lethality, as judged in trypan blue exclusion assays or by Giemsa assays, was first evident ~12 h after drug exposure (data not shown). Alternatively, the Annexin V/propidium iodide assay was carried to determine cell viability according to the manufacturer's instructions (BD Pharmingen, San Diego, CA) using a FACScan flow cytometer (BD Biosciences, San Jose, CA).

Lysotracker Visualization of Lysosomes/Acidic Vacuoles

The Lysotracker Red dye was added at 50 nM (or 75 nM depending on cell type) and incubated for ~20 min. Cells were fixed in 3.4% paraformaldehyde and visualized on an Axiovert 200 fluorescent microscope (Carl Zeiss Inc., Thornwood, NY) under the 40× objective. For 3-methyladenine inhibition of vacuole formation, 5 mM 3 methyl adenine (3MA) was added to the cells for 30 min before OSU-03012 was added. Cells were stained with Lysotracker Red as explained above.

For SDS-PAGE and immunoblotting, cells were plated at 5×10^5 cells/cm^2 and treated with drugs at the indicated concentrations, and after the time of treatment indicated in the legend, lysed in whole-cell lysis buffer (0.5 M Tris-HCl, pH 6.8, 2% SDS, 10% glycerol, 1% β-mercaptoethanol, and 0.02% bromphenol blue), and the samples were boiled for 30 min. The boiled samples were loaded onto 10 to 14% SDS-polyacrylamide gels, and electrophoresis was run overnight. Proteins were electrophoretically transferred onto 0.22-μm nitrocellulose and immunoblotted with various primary antibodies against different proteins. All immunoblots were visualized by ECL. For presentation, immunoblots were digitally scanned at 600 dpi using PhotoShop 7.0 (Adobe Systems, Mountain View, CA) and their color was removed; figures were generated in PowerPoint (Microsoft Corp, Redmond, WA).

Infection of Cells with Recombinant Adenoviruses

Cells were plated at 3×10^3/cm^2 in each well of a 12-well, 6-well, or 60-mm plate. After plating (24 h), cells were infected (at a multiplicity of infection of 50) with a control empty vector virus (CMV) and adenovirus to express HSP70, dominant-negative AKT or dominant-negative mitogen activated extracellular regulated kinase 1 (Vector Biolabs, Philadelphia, PA). Twenty-four hours after infection, cells were treated with indicated concentrations of OSU-03012 and/or drugs, and cell survival or changes in expression/protein phosphorylation were determined 0 to 48 h after drug treatment by trypan blue assay and immunoblotting, respectively.

Transfection of Cells with siRNA or with Plasmids

For Plasmids. Cells were plated as described above and, 24 h after plating, were transfected. For mouse embryonic fibroblasts (2–5 μg) or other cell types (0.5 μg), plasmids expressing a specific mRNA (or siRNA) or appropriate vector control plasmid DNA was diluted in 50 μl of serum-free and antibiotic-free medium (1 portion for each sample). Two microliters of Lipofectamine 2000 (Invitrogen) was concurrently diluted into 50 μl of serum-free and antibiotic-free medium (1 portion for each sample). Diluted DNA was added to the diluted Lipofectamine 2000 for each sample and incubated at room temperature for 30 min. This mixture was added to each well/dish of cells containing 200 μl of serum-free and antibiotic-free medium for a total volume of 300 μl, and the cells were incubated for 4 h at 37°C. An equal volume of 2× medium was then added to each well. Cells were incubated for 48 h and then treated with OSU-03012. For analysis of cells transfected with GFP-LC3 constructs, the GFP-LC3-positive vacuolated cells were examined under the 40× objective of a Zeiss Axiovert fluorescent microscope. Forty LC3-GFP-positive cells were analyzed per condition. Each vacuole was counted, and the average number of vacuoles per cell for each, including cells that did not exhibit vacuolization, was calculated.

For HSP70 Promoter-Luciferase Assays. Cells, MEFs or U251, were plated as described above and, 24 h after plating, were transfected with either a control luciferase plasmid (1 μg) + β-galactosidase (β-Gal) plasmid (15 ng), or Luciferase plasmid (1 μg) + β-Gal plasmid (15 ng) were incubated for 5 min in serum-free medium, then added to Gene Juice (2 μl/condition; EMD Biosciences, San Diego, CA), and incubated 15 min together at room temperature (Yacoub et al., 2004). This mixture was added to cells and incubated at 37°C for 24 h, after which cells were treated with OSU-03012 for 0 to 24 h, washed twice with phosphate-buffered saline, and harvested in cell lysis buffer [25 mM Tris phosphate, pH 7.8, 2 mM dithiothreitol, 2 mM CDTA, 10% glycerol, and 1% (v/v) Triton X-100]. The lysate was centrifuged for 5 min at 13,000g at 4°C to pellet debris. The luciferase assay was performed according to the manufacturer's instructions (Promega, Madison, WI). In brief, luciferase substrate was brought to room temperature, then added to 20 μl of lysate and measured immediately on a PerkinElmer luminometer. The luciferase measurement was normalized to β-Galactosidase measurement to control for transfection efficiency; 50 μl of 2× β-galactosidase reagent (200 mM Na$_2$HPO$_4$/NaH$_2$PO$_4$, pH7.4, 2 mM MgCl$_2$, 200 mM β-mercaptoethanol, 1.34 mg/ml O-nitrophenyl-β-D-galactopyranoside) was added to 50 μl of cell lysate and incubated at 37°C for 10 min. The product of the assay was measured at OD$_{405}$.

Fig. 1. OSU-03012 toxicity in transformed cells is mediated in part via cathepsin B-BID-AIF signaling. A, HCT116 cells were transiently transfected as described under *Materials and Methods* 24 h after plating with either a scrambled siRNA (siSCR) or an siRNA against AIF (siAIF) (12). Forty-eight hours after transfection, cells were treated with the pan-caspase inhibitor zVAD (50 μM); 30 min later, cells were treated with vehicle (VEH, DMSO) or with OSU-03012 (OSU, 1 μM, 3 μM). Cells were isolated by trypsinization 48 h after drug treatments. Cell viability was determined using a trypan blue exclusion assay in triplicate. Data are from a representative experiment ($n = 3$). (∗, $p < 0.05$ less than corresponding siSCR value). Inset, cells were isolated 24 h after vehicle or OSU-03012 treatment and subjected to SDS-PAGE followed by immunoblotting for AIF performed. B, U251 cells were stably transfected with either a scrambled siRNA (siSCR) or an siRNA against AIF (siAIF) (see inset immunoblotting panel). Cells, 24h after plating, were treated with vehicle (VEH, DMSO) or with OSU-03012 (OSU, 1 μM, 2 μM, 5 μM). Cells were isolated by trypsinization 48h after drug treatments. Cell viability was determined using a trypan blue exclusion assay in triplicate. Data are from a representative experiment ($n = 3$). (∗, $p < 0.05$ less than corresponding siSCR value). Similar data were observed in multiple individual clones of these transfected U251 cells (data not shown). C, MEFs were treated with vehicle (DMSO) or with OSU-03012 (1–3 μM). Cells were isolated by trypsinization 48 h after drug treatment. Cell viability was determined using a trypan blue exclusion assay in triplicate. Data are from a representative experiment ($n = 3$). (∗, $p < 0.05$ less than corresponding value in wild-type fibroblasts). D, left, immortal MEFs, either WT or cathepsin B$^{-/-}$, were cultured as described under *Materials and Methods*. Twenty-four hours after plating cells were treated with vehicle (VEH, DMSO) or with OSU-03012 (OSU, 1 μM). Cells were isolated by trypsinization at the indicated times after drug treatments and immunoblotting was performed to determine the cleavage status of BID in each cell line. A representative study is shown ($n = 3$). Right, MEFs, either WT, BID$^{-/-}$, or cathepsin B$^{-/-}$ (Cath. B$^{-/-}$), were cultured as described under *Materials and Methods*. Twenty-four hours after plating cells were treated with vehicle (VEH, DMSO) or with OSU-03012 (OSU, 1 μM). Cells were isolated by trypsinization 6 h after OSU-03012 treatment, and the cytosolic fraction was isolated as described under *Materials and Methods*. Immunoblotting was performed to determine the release of AIF into the cytosol after OSU-03012 treatment. A representative study is shown ($n = 3$).
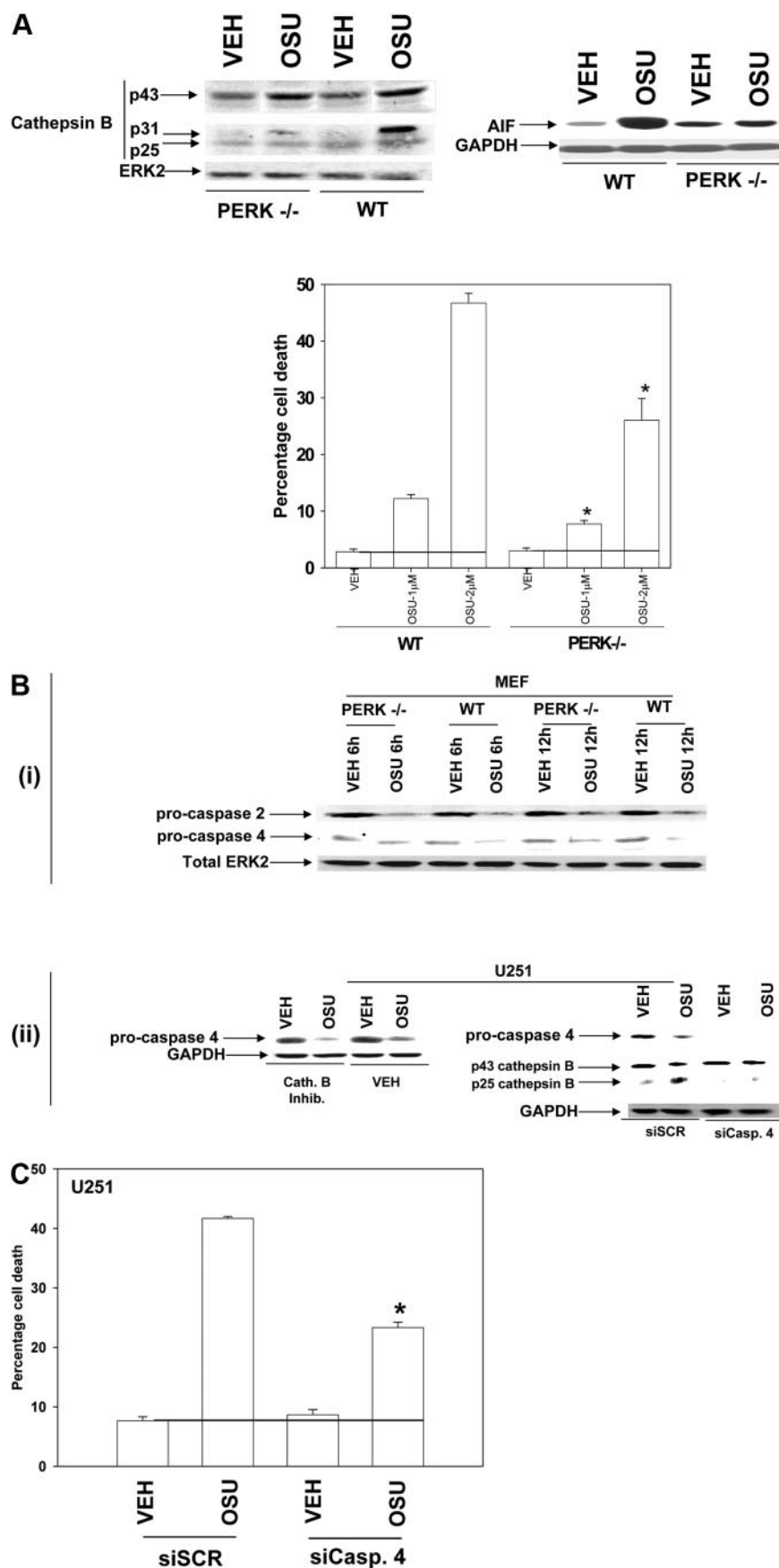
Fig. 2. OSU-03012 toxicity is reduced in PERK$^{-/-}$ fibroblasts and in cells lacking caspase 4 function. A, transformed WT and PERK$^{-/-}$ MEFs were cultured as described under *Materials and Methods*. Twenty-four hours after plating, cells were treated with vehicle (VEH, DMSO) or with OSU-03012 (OSU, 0–2 μM). Top left, 6 hours after OSU-03012 exposure (1 μM), cells were isolated and the total cell lysate was immunoblotted to determine the expression and cleavage status of cathepsin B. Top right, 6 hours after OSU-03012 exposure (1 μM), cells were isolated and hours after OSU-03012 exposure, cells were isolated and cytosolic fraction obtained. The release of AIF into the cytosol after OSU-03012 exposure was determined by immunoblotting. Bottom, transformed WT and PERK$^{-/-}$ MEFs were isolated by trypsinization 24 h after drug treatment. Cell viability was determined using a trypan blue exclusion assay in triplicate. Data are from a representative experiment ($n = 3$). (∗, $p <$ 0.05 less than value in WT cells). B, i, transformed WT and PERK$^{-/-}$ MEFs were cultured as described under *Materials and Methods*. Twenty-four hours after plating, cells were treated with vehicle (VEH, DMSO) or with OSU-03012 (OSU, 1 μM). Six and 12 h after drug treatment, cells were isolated and the total cell lysate was immunoblotted to determine the expression of pro-caspase 2 and pro-caspase 4. Data are from a representative experiment ($n = 3$). ii, left, U251 cells were cultured as described under *Materials and Methods*. Twenty-four hours after plating, cells were treated with vehicle (DMSO) or the cathepsin B inhibitor (cath. B inhib., 1 μM); 30 min later, they were treated with vehicle (VEH, DMSO) or with OSU-03012 (OSU, 1 μM). Cells were isolated by trypsinization 12 h after drug treatment, and immunoblotting was performed to determine the expression of pro-caspase 4. ii, right, U251 cells were transiently transfected as described under *Materials and Methods* 24 h after plating with either a scrambled siRNA (siSCR) or an siRNA against caspase 4 (sicaspase4). Forty-eight hours after transfection, cells were treated, where indicated, with the cathepsin B inhibitor (cath. B inhib.); 30 min later, cells were treated with vehicle (VEH, DMSO) or with OSU-03012 (OSU, 1 μM). Cells were isolated by trypsinization 12 h after drug treatments, and the total cell lysate was immunoblotted to determine the expression of cathepsin B and pro-caspase 4. Data are from a representative experiment ($n = 3$). C, U251 cells were transiently transfected as described under *Materials and Methods* 24 h after plating with either a scrambled siRNA (siSCR) or an siRNA against caspase 4 (sicaspase4). Forty-eight hours after transfection, cells were treated, where indicated, with vehicle (VEH, DMSO) or with OSU-03012 (OSU, 1 μM). Cells were isolated by trypsinization 48 h after drug treatments and cell viability was determined using a trypan blue exclusion assay in triplicate. Data are from a representative experiment ($n = 3$). (∗, $p <$ 0.05 less than corresponding value in siSCR-transfected cells).
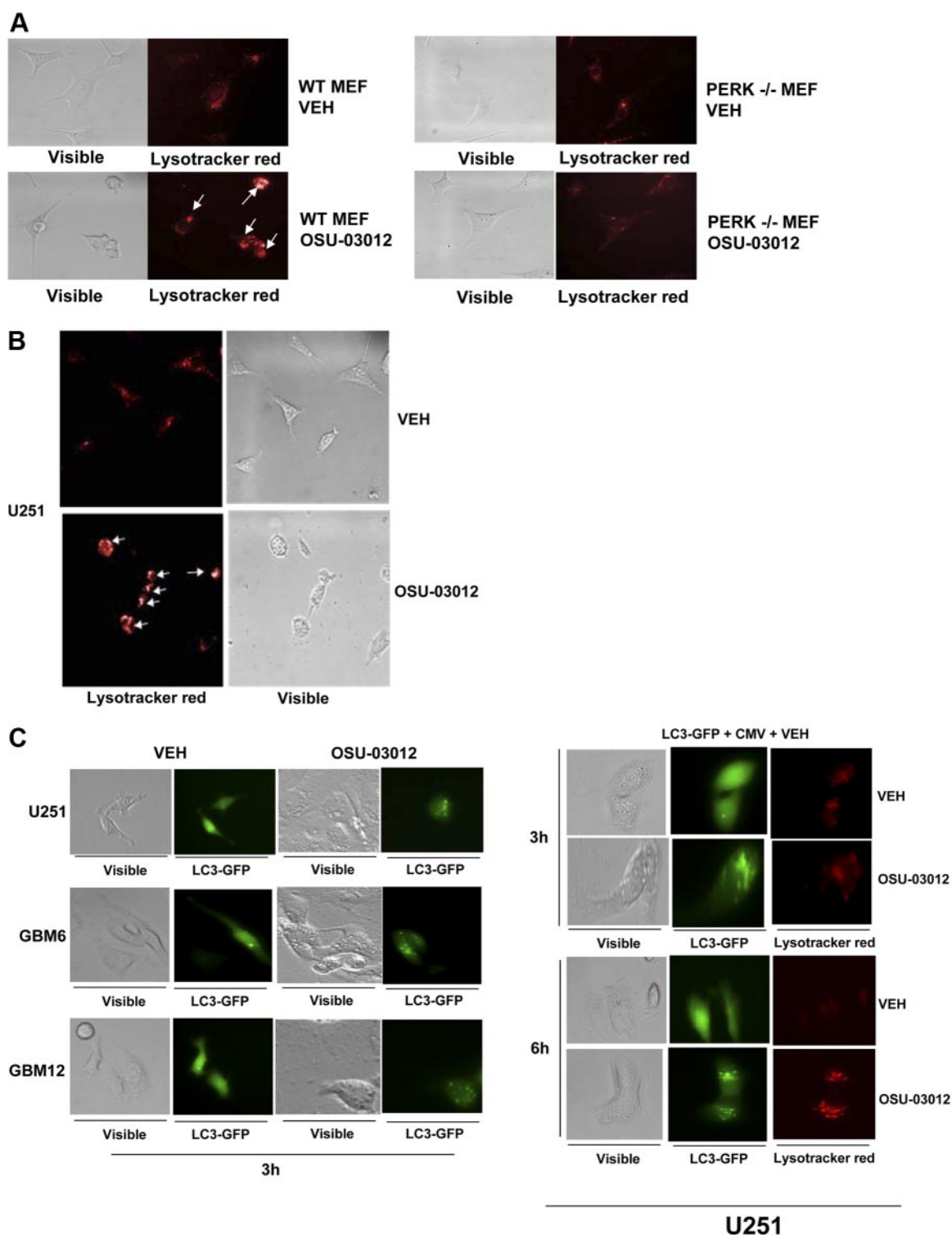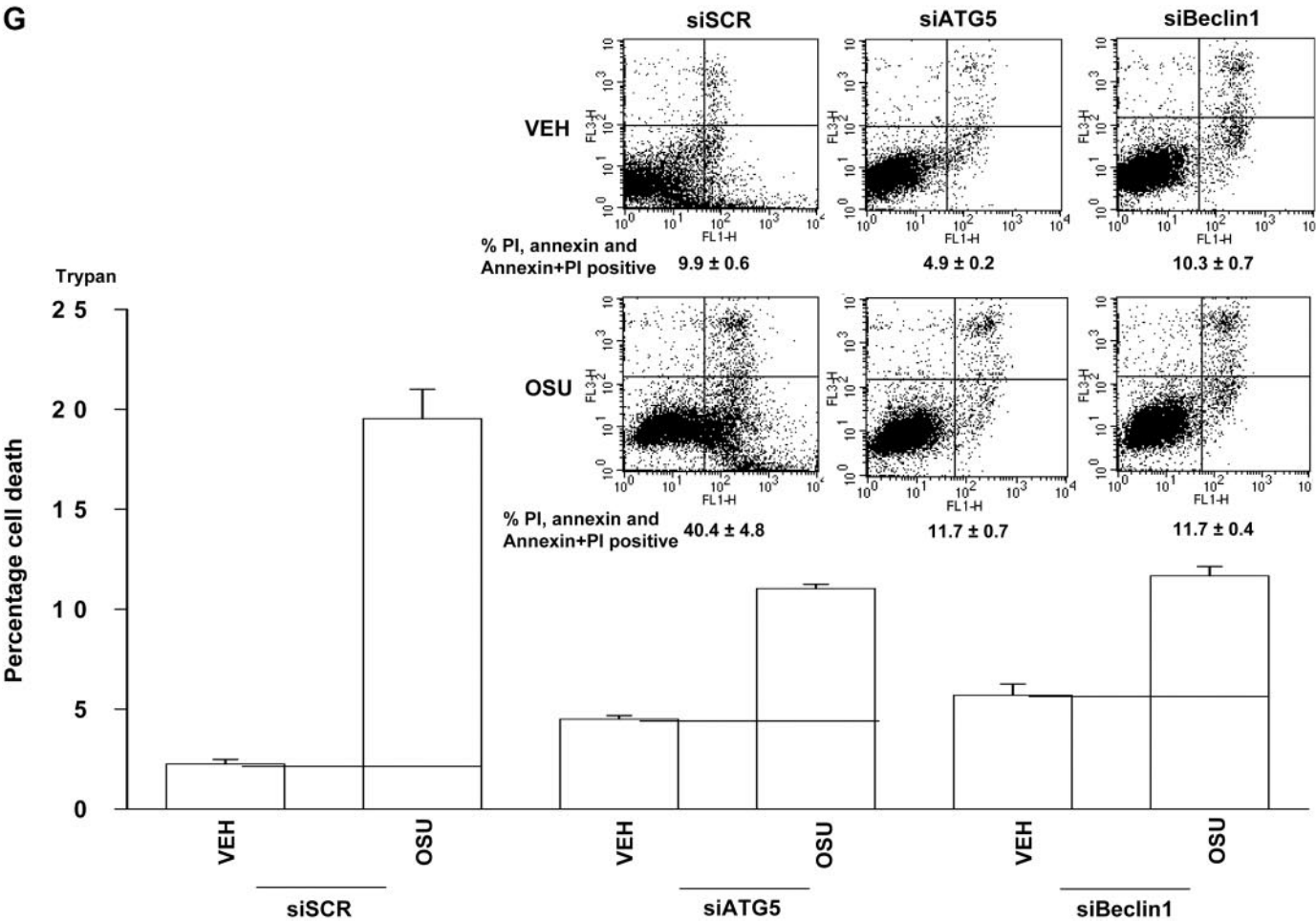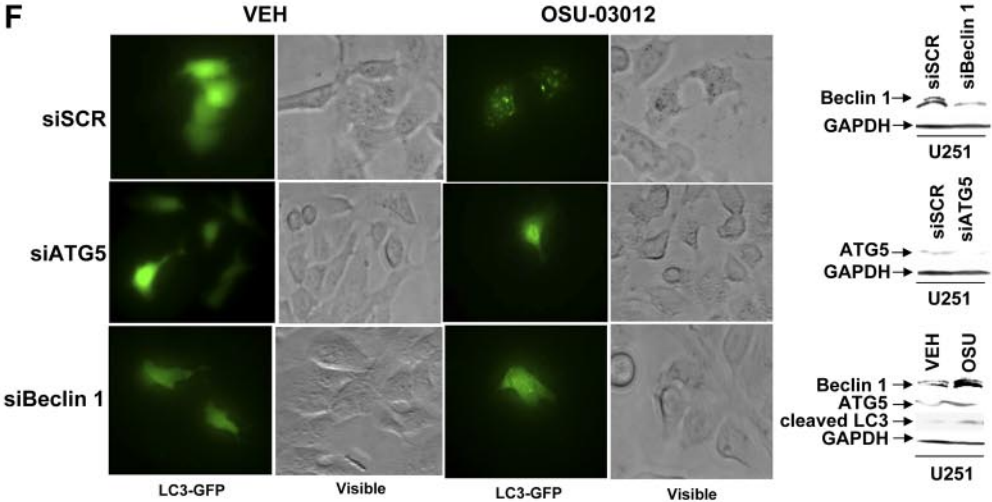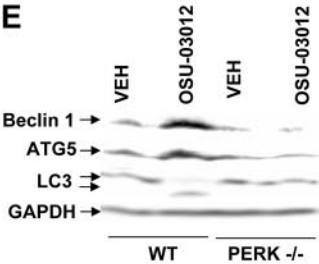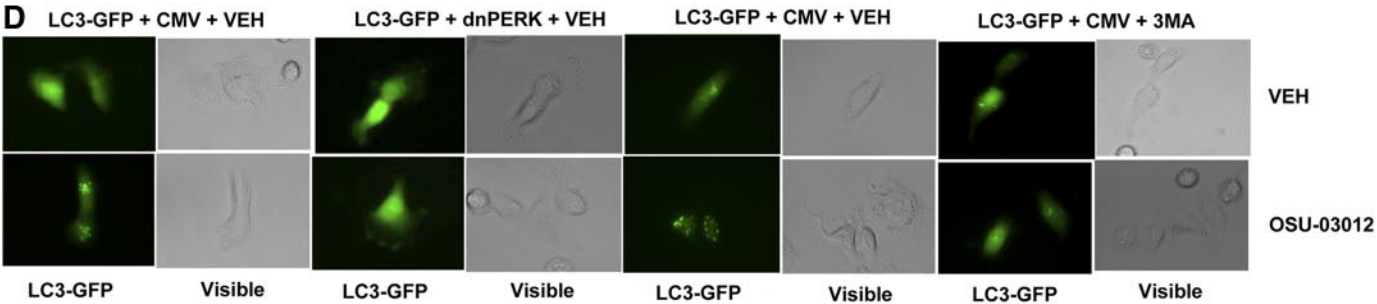
Fig. 3. OSU-03012 causes vacuolization of low pH vesicles and LC3 containing vesicles in transformed cells. A, transformed WT MEF, WT, and PERK$^{-/-}$ were plated in four-chamber glass slides and 24 h later treated with vehicle (DMSO) or with OSU-03012 (1 μM). Cells were fixed 6 h after drug exposure and stained with Lysotracker Red dye. Cells were visualized at 40× using an Axiovert 200 fluorescent microscope under fluorescent light and visible light. Data shown is a representative field from one experiment (n = 3). White arrows denote areas of intense staining, indicative of vacuolization. B, U251 cells were plated in four-chamber glass slides and 24 h later treated with vehicle (DMSO) or with OSU-03012 (1 μM). Cells were fixed 6 h after drug exposure and stained with Lysotracker Red dye. Cells were visualized at 40× using an Axiovert 200 fluorescent microscope under fluorescent light and visible light. Data shown is a representative field from one experiment (n = 3). White arrows denote areas of intense staining, indicative of vacuolization. C, U251, GBM6, and GBM12 cells were plated in four-chamber glass slides and 24 h later transfected with an empty vector plasmid or a plasmid to express a GFP-tagged form of LC3. Twenty-four hours after transfection, cells were treated with vehicle (DMSO) or with OSU-03012 (1 μM). Three and 6 h after OSU-03012 treatment, as indicated, cells were stained, where indicated, with Lysotracker Red dye and the cells were visualized at 40X using an Axiovert 200 fluorescent microscope under fluorescent light (Lysotracker Red dye-stained cells were visualized immediately after staining on a Zeiss Axiovert 200 microscope using the rhodamine filter). LC3-GFP transfected cells were visualized at the indicated 3- and 6-h time points on the Zeiss Axiovert 200 microscope using the FITC filter and under visible light. Data shown is a representative field from one experiment (n = 3).

D

LC3-GFP + CMV + VEH   LC3-GFP + dnPERK + VEH   LC3-GFP + CMV + VEH   LC3-GFP + CMV + 3MA

VEH

OSU-03012

LC3-GFP   Visible   LC3-GFP   Visible   LC3-GFP   Visible   LC3-GFP   Visible

E

Beclin 1 →
ATG5 →
LC3 →
GAPDH →

VEH   OSU-03012   VEH   OSU-03012

WT   PERK -/-

F

VEH   OSU-03012

siSCR

siATG5

siBeclin 1

LC3-GFP   Visible   LC3-GFP   Visible

Beclin 1 →   siSCR   siBeclin 1
GAPDH →
U251

ATG5 →   siSCR   siATG5
GAPDH →
U251

Beclin 1 →   VEH   OSU
ATG5 →
cleaved LC3 →
GAPDH →
U251

G

siSCR   siATG5   siBeclin1

VEH

OSU

% PI, annexin and
Annexin+PI positive   9.9 ± 0.6   4.9 ± 0.2   10.3 ± 0.7

% PI, annexin and
Annexin+PI positive   40.4 ± 4.8   11.7 ± 0.7   11.7 ± 0.4

Trypan

Percentage cell death

VEH   OSU   VEH   OSU   VEH   OSU
siSCR   siATG5   siBeclin1

Transfection with siRNA. Cells were plated in 60-mm dishes from a fresh culture growing in log phase as described above and, 24 h after plating, were transfected. Before transfection, the medium was aspirated, and 1 ml of serum-free medium was added to each plate. For transfection, 10 nM concentrations of the annealed siRNA targeting AIF, ATG5, Beclin 1, caspase 4, or HSP70, the positive sense control doubled-stranded siRNA targeting glyceraldehyde-3-phosphate dehydrogenase, or the negative control (a "scrambled" sequence with no significant homology to any known gene sequences from mouse, rat or human cell lines) were used (predominantly Qiagen; occasional alternate siRNA molecules were purchased from Ambion, Inc., Austin, TX). Ten nanomolar siRNA (scrambled or experimental) was diluted in serum-free media. Four microliters of Hiperfect (QIAGEN) was added to this mixture, and the solution was mixed by pipetting up and down several times. This solution was incubated at room temperature for 10 min, then added dropwise to each dish. The medium in each dish was swirled gently to mix, then incubated at 37°C for 2h. One milliliter of 10% (v/v) serum-containing medium was added to each plate, and cells were incubated at 37°C for 48 h before re-plating (50×10^3 cells each) onto 12-well plates. Cells were allowed to attach overnight, then treated with OSU-03012 (0–48 h). Trypan blue exclusion assays and SDS-PAGE/immunoblotting analyses were then performed at the indicated time points (Yacoub et al., 2004; Carón et al., 2005).

Manipulation of Drug-Treated Cells to Isolate a Crude Cytosolic Fraction. A crude membrane fraction was prepared from treated cells as described by Yacoub et al. (2006). In brief, cells were washed twice in ice-cold isotonic HEPES buffer (10 mM HEPES, pH 7.5, 200 mM mannitol, 70 mM sucrose, 1 μM EGTA, and 10 μM protease inhibitor cocktail) (Sigma, St. Louis, MO). Cells on ice were scraped into isotonic HEPES buffer and lysed by passing 20 times through a 25-gauge needle. Large membrane pieces, organelles, and unlysed cells were removed from the suspension by centrifugation for 5 min at 120g. The crude granular fraction and cytosolic fraction was obtained from by centrifugation for 30 min at 10,000g, leaving the cytosol as supernatant.

Data Analysis. Comparison of the effects of various treatments was performed after analysis of variance using the Student's t test. Differences with a p value of <0.05 were considered statistically significant. Experiments shown are the means of multiple individual points ($\pm$ S.E.M.).

Results

Treatment of HCT116 and U251 human tumor cells with OSU-03012 caused a dose-dependent induction of cell death that was suppressed by use of multiple transient or stable siRNA molecules to knock down AIF expression and inhibition of cathepsin function but was not altered by incubation

with the "pan"-caspase inhibitor zVAD (Fig. 1, A and B) (Yacoub et al., 2006; Hart et al., 2007). Previously we demonstrated that OSU-03012 lethality correlated with increased release of cathepsin B into the cytosol as well as its cleavage into active forms, as judged using a small molecule cathepsin inhibitor (Yacoub et al., 2006). One potential mechanism by which OSU-03012 could cause AIF release into the cytosol via cathepsin B activation was by promoting the cleavage of BID, and we noted previously that the lethality of OSU-03012 was suppressed in transformed BID$^{-/-}$ transformed fibroblasts (Yacoub et al., 2006). In the present studies, we demonstrate that OSU-03012 lethality was also suppressed in cathepsin B$^{-/-}$ fibroblasts as judged in trypan blue and Annexin-PI staining assays that correlated with reduced OSU-03012–stimulated cleavage of BID and reduced release of AIF into the cytosol (Fig. 1, C and D).

Overexpression of either BCL-XL or BCL-2 can protect mitochondria, as well as the ER, from toxic stresses and the parent compound of OSU-03012, celecoxib, has been proposed to use ER stress to kill malignant cells (Fehrenbacher et al., 2004). We have noted that overexpression of BCL-XL modestly suppressed the toxicity of OSU-03012 in human glioma cells, and others have noted that overexpression of BCL-2 in malignant hematologic cells did not suppress OSU-03012 toxicity (Tseng et al., 2005, 2006; Yacoub et al., 2006; To et al., 2007). We also found in PERK-null (PERK$^{-/-}$) fibroblasts that the ability of OSU-03012 to cause cell death was significantly reduced, whereas the toxicity of thapsigargin was enhanced in PERK$^{-/-}$ cells (Fig. 2A, data not shown) (Yacoub et al., 2006). OSU-03012–induced release of AIF into the cytosol and cleavage of cathepsin B were PERK-dependent (Fig. 2A, upper immunoblotting panels). Identical cell survival data were obtained when a truncated dominant-negative PERK protein was stably expressed in K562 leukemic cells treated with OSU-03012 (data not shown). In contrast to loss of PERK function, expression of a dominant-negative eIF2α protein (eIF2α S51A) did not significantly alter the toxicity of OSU-03012 in 3T3 fibroblasts [data not shown (Yacoub et al., 2006)].

Pro-apoptotic ER stress signaling downstream of PERK-eIF2α-CHOP and IRE-CHOP has been linked in a variety of cell types to changes in the activities of pro-caspase 12, pro-caspase 2, and pro-caspase 4, enzymes that can also directly promote BID cleavage/mitochondrial dysfunction and that can thus also directly activate the intrinsic apoptosis path-

Fig. 3, *continued.* D, U251 cells were plated in four-chamber glass slides and 24 h later treated transfected with an empty vector plasmid or a plasmid to express a GFP-tagged form of LC3. In parallel, the cells were transfected with an empty vector plasmid or a plasmid to express a truncated dominant-negative form of PERK. Twenty-four hours after transfection, cells were pretreated with vehicle (veh, phosphate-buffered saline) or 3-methyl adenine (5 mM) followed 30 min later by vehicle (VEH, DMSO) or with OSU-03012 (OSU, 1 μM). Six hours after OSU-03012 treatment, cells were visualized at 40$\times$ using an Axiovert 200 fluorescent microscope under fluorescent light on the Zeiss Axiovert 200 microscope using the FITC filter and under visible light. Data shown is a representative field from one experiment ($n = 3$). E, transformed WT mouse embryonic fibroblasts, WT, or PERK$^{-/-}$, were plated and 24 h later treated with vehicle (DMSO) or with OSU-03012 (1 μM). Cells were isolated 6 h after drug exposure, and the total cell lysate was immunoblotted to determine the expression of Beclin 1, ATG5, and LC3. Data shown are representative of one experiment ($n = 3$). F, U251 cells were plated in four-chamber glass slides and 24 h later transfected with an empty vector plasmid or a plasmid to express a GFP-tagged form of LC3. In parallel, the cells were transfected with an empty vector plasmid expressing a scrambled siRNA sequence (siSCR) or with plasmids to express siRNAs to suppress the expression of Beclin 1 (siBeclin 1) or to suppress expression of ATG5 (siATG5). Forty-eight hours after transfection, cells were treated with vehicle (VEH, DMSO) or with OSU-03012 (OSU, 1 μM). Six hours after OSU-03012 treatment, cells were visualized at 40$\times$ using an Axiovert 200 fluorescent microscope under fluorescent light on the Zeiss Axiovert 200 microscope using the FITC filter and under visible light. Data shown is a representative field from one experiment ($n = 3$). In parallel studies, inset to right, cells were isolated 6 h after drug exposure, and total cell lysates were immunoblotted to determine the expression of Beclin 1, ATG5, and LC3 after OSU-03012 treatment and in cells transfected with the siBeclin 1 and with the siATG5 constructs. Data shown is a representative field from one experiment ($n = 3$). G, U251 cells were plated in four-chamber glass slides and 24 h later transfected with an empty vector plasmid expressing a scrambled siRNA sequence (siSCR) or with plasmids to express siRNAs to suppress the expression of Beclin 1 (siBeclin 1) or to suppress expression of ATG5 (siATG5). Forty-eight hours after transfection, cells were treated with vehicle (VEH, DMSO) or with OSU-03012 (OSU, 1 μM). Cells were isolated by trypsinization 48 h after drug treatments, and cell viability was determined using a trypan blue exclusion assay in triplicate. Data are from a representative experiment ($n = 3$). ($*$, $p < 0.05$ less than corresponding value in siSCR-transfected cells).

way (reviewed in Hitomi et al., 2004; Yeung et al., 2006). Caspases 2 and 4 have been noted to be relatively refractory to the protective actions of the "pan"-caspase inhibitor zVAD (Ekert et al., 1999). OSU-03012 promoted pro-caspase 4 degradation, which was suppressed in PERK$^{-/-}$ MEFs and caused pro-caspase 2 degradation that was largely PERK-independent [Fig. 2B, upper inset panel (i)]. Transient knockdown of caspase 4 expression using a short hairpin RNA in U251 cells suppressed OSU-03012 toxicity. It is noteworthy that after OSU-03012 treatment, loss of caspase 4 expression suppressed cathepsin B cleavage and inhibition of cathepsin B activity did not alter OSU-03012–induced cleavage of pro-caspase 4; indeed, inhibition of cathepsin B seemed to promote caspase 4 activation [Fig. 2, B and C, lower inset panel (ii)]. Similar data were obtained after OSU-03012 treatment in cathepsin B$^{-/-}$ fibroblasts and in HCT116 cells and also in U251 and U937 cells with knockdown of pro-caspase 4 expression using a plasmid expressed siRNA molecule (data not shown; Rahmani et al., 2007).

Cathepsin B is localized in endosomes in resting glioma cells, and this enzyme plays a role in cell migration, angiogenesis, and cell death processes (Lakka et al., 2005). Because OSU-03012 caused cathepsin B release into the cytosol and proteolytic cleavage of cathepsin B, and endosomal dysfunction has been linked to cell death processes, we determined whether endosome function was altered by OSU-03012 treatment. OSU-03012 caused vacuolization of acidic endosomes in transformed MEFs within 6 h of exposure, as judged by intense Lysotracker Red staining that was almost an all or nothing effect (Fig. 3A). OSU-03012 did not cause vacuolization of acidic endosomes in PERK$^{-/-}$ MEFs or in wild-type MEFs treated with a nonspecific autophagy inhibitor, 3MA (Fig. 3A, data not shown). Similar data were also obtained in U251, GBM6, and GBM12 human cancer cells (Fig. 3B, data not shown).

Vacuolization of the protein LC3 is one recognized marker for autophagy, and transfection of U251 glioma cells with a construct to express a GFP-tagged LC3 protein demonstrated that OSU-03012 treatment induced vacuolization of GFP-tagged LC3 within 3 h (Fig. 3C); the appearance of LC3-GFP positive vacuoles preceded Lysotracker Red staining of acidic endosomes by ~3 h (Fig. 3C) (Seglen and Bohley, 1992; Dunn, 1994; Kabeya et al., 2000). Expression of dominant-negative PERK in glioma cells or treatment of these cells with 3MA significantly suppressed OSU-03012–induced vac-

uolization of the LC3-GFP protein, as well as the induction of acidic endosomes (Fig. 3D, Table 1, data not shown).

The ATG12-ATG5 and the ATG8 (LC3)-PE conjugation systems are interdependent, and a disruption in one system has a direct negative effect on the autophagic process (Levine et al., 2005; Yang et al., 2005; Shibata et al., 2006; Yousefi et al., 2006). Beclin-1 is a functional component of the lipase signaling complex, which is essential for the induction of autophagy (Levine et al., 2005; Yang et al., 2005; Shibata et al., 2006; Yousefi et al., 2006). Therefore, perturbation of the levels of ATG5 or Beclin-1 should result in reduced autophagy, and the attenuation of the biological effects of OSU. To test this, differing short hairpin and plasmid expressed RNA interference approaches were used to specifically suppress ATG5 and Beclin-1 protein levels in tumor cells. Cells were transiently transfected with short hairpin RNA constructs targeting ATG5 or Beclin-1. OSU-03012 treatment rapidly increased the expression of ATG5, and caused rapid complete cleavage of endogenous LC3 protein in U251 and in wild-type MEFs; the OSU-03012–stimulated elevation of ATG5 expression and LC3 cleavage were not present in PERK$^{-/-}$ MEFs (Fig. 3, E and F). Knock down of ATG5 or Beclin 1 expression in U251 cells significantly suppressed the appearance of LC3-positive vacuoles in glioma cells after OSU-03012 treatment (Fig. 3E, Table 2; data not shown). Knock down of Beclin 1 or ATG5 expression suppressed the toxicity of OSU-03012 in glioma cells (Fig. 3G, data not shown).

We next attempted to place the activation of cathepsin B within the context of OSU-03012–induced vacuolization. Loss of cathepsin B expression abolished OSU-03012–induced acidic endosome vacuolization but did not alter the ability of OSU-03012 to cause LC3-GFP vacuolization. These data provide support for the argument that that the apparent secondary Lysotracker Red staining/acidic endosome vacuolization after OSU-03012 exposure was a cathepsin B-dependent process (Fig. 4). Together, our data demonstrate that OSU-03012 causes a PERK-dependent induction of ATG5 and Beclin 1 expression that causes the formation of vacuoles that contain LC3; these data suggest that OSU-03012 causes an autophagic response in glioma cells and in rodent fibroblasts.

Based on the observation that OSU-03012 caused cell death, in part, via endosomal dysfunction, as well as via AIF release into the cytosol (Yacoub et al., 2006), we examined

TABLE 1

Expression of dominant-negative PERK or treatment with 3MA suppresses the formation of GFP-LC3 containing vacuoles after OSU-03012 exposure

U251 cells were plated in four-chamber glass slides and 24 h later transfected with an empty vector plasmid or a plasmid to express a GFP-tagged form of LC3. In parallel, the cells were transfected with an empty vector plasmid or a plasmid to express a truncated dominant negative form of PERK. Twenty-four hours after transfection, cells were pretreated with vehicle (veh, PBS) or 3MA (5 mM) followed 30 min later by vehicle (VEH, DMSO) or with OSU-03012 (OSU, 1 μM). Six hours after OSU-03012 treatment, cells were visualized at 40$\times$ using an Axiovert 200 fluorescent microscope under fluorescent light, on the Zeiss Axiovert 200 microscope using the FITC filter, and under visible light. Data shown is from 40 transfected cells from a representative experiment ($n = 3$). Mean autophagic vesicles per U251 cell 24 h after treatment ($n = 40$ LC3.GFP-transfected cells $\pm$ S.E.M.).

CMV		dn PERK		3MA	
+ VEH	+ OSU	+ VEH	+ OSU	+ VEH	+ OSU
2.0 ± 0.7	7.6 ± 1.2	1.3 ± 0.4	1.5 ± 0.3*	1.1 ± 0.3	1.2 ± 0.3*

dn, dominant negative.
* $p < 0.05$ less than parallel value in CMV-transfected cells.

TABLE 2

Knockdown of Beclin 1 or ATG5 expression suppresses OSU-03012–induced formation of GFP-LC3 vacuoles in U251 cells

U251 cells were plated in four-chamber glass slides and 24 h later transfected with an empty vector plasmid or a plasmid to express a GFP-tagged form of LC3. In parallel, the cells were transfected with an empty vector plasmid expressing a scrambled siRNA sequence (siSCR) or with plasmids to express siRNAs to suppress the expression of Beclin 1 (siBeclin 1) or to suppress expression of ATG5 (siATG5). Forty-eight hours after transfection cells were treated with vehicle (VEH, DMSO) or with OSU-03012 (OSU, 1 μM). Six hours after OSU-03012 treatment, cells were visualized at 40$\times$ using an Axiovert 200 fluorescent microscope under fluorescent light, on the Zeiss Axiovert 200 microscope using the FITC filter, and under visible light. Data shown is from 40 transfected cells from a representative experiment ($n = 3$). Mean autophagic vesicles per U251 cell 24 h after treatment ($n = 40$ LC3.GFP-transfected cells $\pm$ S.E.M.).

SiSCR		siATG5		siBECLIN 1	
+ VEH	+ OSU	+ VEH	+ OSU	+ VEH	+ OSU
1.6 ± 0.6	9.9 ± 1.6#	0.6 ± 0.2	3.4 ± 0.7*	1.2 ± 0.4	3.5 ± 0.8*

* $p < 0.05$ less than parallel value in SiSCR-transfected cells.
# $p < 0.05$ greater than VEH.

whether any of these effects correlated with any parallel compensatory alterations in the expression of a protein whose functions could ameliorate the pro-apoptotic actions of such events (i.e., HSP70) (Mosser et al., 2000; Ravagnan et al., 2001; Gurbuxani et al., 2003; Nylandsted et al., 2004; Demidenko et al., 2006; Mambula and Calderwood, 2006). Treatment of transformed MEFs with OSU-03012 rapidly increased HSP70 expression and decreased HSP90 expression, effects that were PERK-dependent (Fig. 5, A, (i) and (ii), and B). After ~6 to 9 h of OSU-03102 exposure, expression of BiP/Grp78 surprisingly began to decline, contrary to a "classic" ER stress response, whereas expression of Grp94 and CHOP variably changed from experiment to experiment (Fig. 5A, data not shown) (Ron, 2002; Rutkowski and Kaufman, 2004). The increase in HSP70 protein expression in cells was not due to altered rates of transcription; in fibroblasts and U251 cells, OSU-03012 treatment caused a modest albeit significant reduction in the activity of the HSP70 promoter (Fig. 5C).

Based on data in Fig. 5A, we determined whether changes in HSP70 function altered the toxicity of OSU-03012 using NZ28, an established small-molecule inhibitor of HSP70 function. Treatment of U251 glioma cells and transformed rodent fibroblasts with NZ28 enhanced the toxicity of OSU-03012, suggesting that inhibition of HSP70 function could promote OSU-03012 toxicity (Fig. 5D). Because HSP70 inhibits AIF function, and to determine one potential protective site of HSP70 action, we made further use of U251 cells lacking AIF expression (Ravagnan et al., 2001; Gurbuxani et al., 2003; Hart et al., 2007). Inhibition of HSP70 with NZ28 enhanced OSU-03012 toxicity in vector control siRNA expressing U251 cells in a dose-dependent, fashion but did not enhance OSU-03012 toxicity in U251 cells lacking AIF expression [Fig. 5E (see also Fig. 1B)]. This suggests that at least one mechanism of HSP70 action in protecting cells from OSU-03012 toxicity is by blocking the proapoptotic actions of AIF.

To extend our findings, we performed further studies using molecular approaches and determined that transient knockdown of HSP70 expression increased, and overexpression of HSP70 decreased, the toxicity of OSU-03012 in HCT116 and U251 tumor cells (Figs. 6, A-D; data not shown). Similar data were obtained using an additional siRNA molecule to knock down HSP70 expression (data not shown). We next determined whether overexpression of HSP70 altered OSU-03012–induced acidic endosome vacuolization (Nylandsted et al., 2004; Mambula and Calderwood, 2006). Overexpression of HSP70 suppressed the low pH endosome vacuolization response of OSU-03012–treated HCT116 and U251 cells as judged microscopically (Fig. 6C, inset). Overexpression of
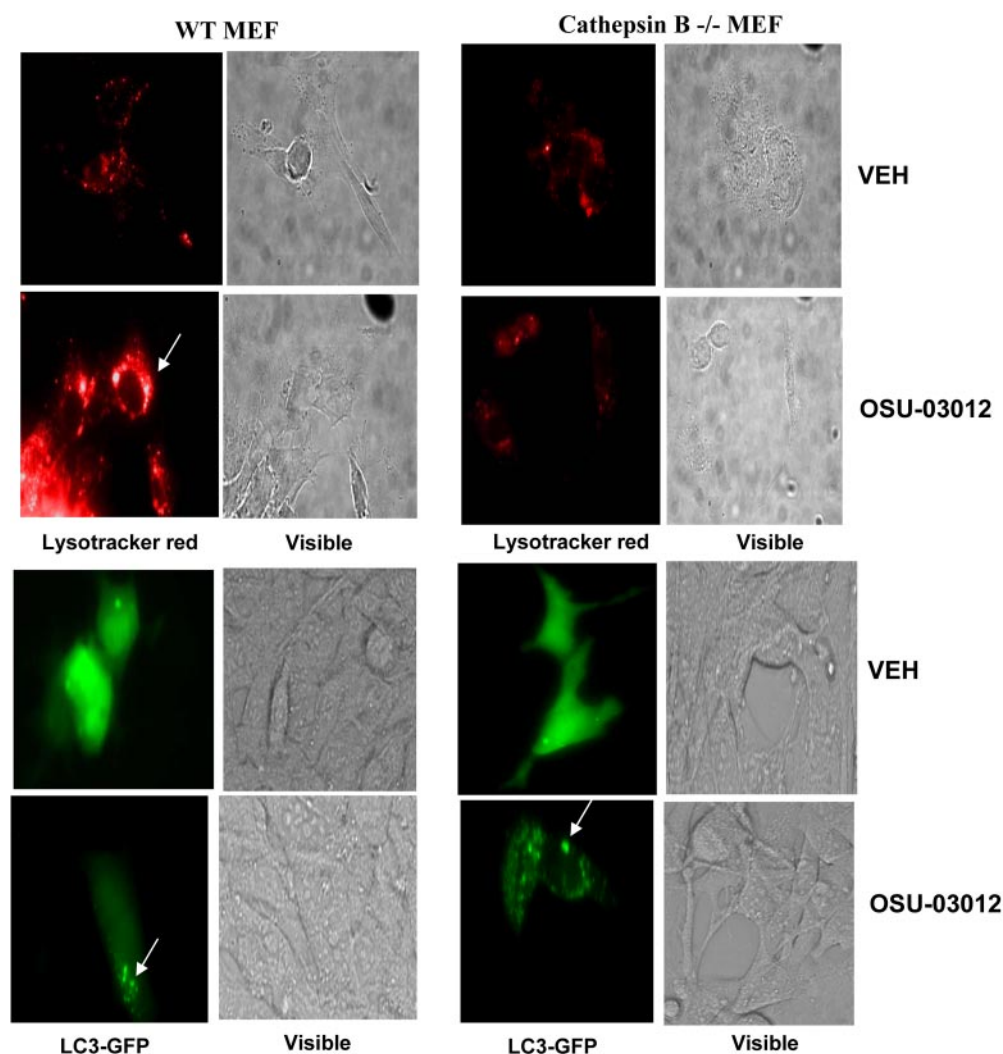

Fig. 4. Loss of cathepsin B expression abolishes OSU-03012–induced acidic endosome formation but not GFP-LC3 vacuolization. Immortal MEFs, either WT or cathepsin B$^{-/-}$, were cultured as described under *Materials and Methods*. Twenty-four hours after plating, cells were transfected with an empty vector plasmid or a plasmid to express a GFP-tagged form of LC3. Twenty-four hours after transfection, cells were treated with vehicle (DMSO) or with OSU-03012 (1 μM). Six hours after OSU-03012 treatment, cells were stained where indicated with Lysotracker Red, and the cells were visualized at 40$\times$ using an Axiovert 200 fluorescent microscope under fluorescent light (Lysotracker Red dye-stained cells were visualized immediately after staining on a Zeiss Axiovert 200 microscope using the rhodamine filter. LC3-GFP transfected cells were visualized at the indicated time points on the Zeiss Axiovert 200 microscope using the FITC filter and under visual light. Data shown is a representative field from one experiment (n = 3). White arrows denote areas of intense staining, indicative of vacuolization.
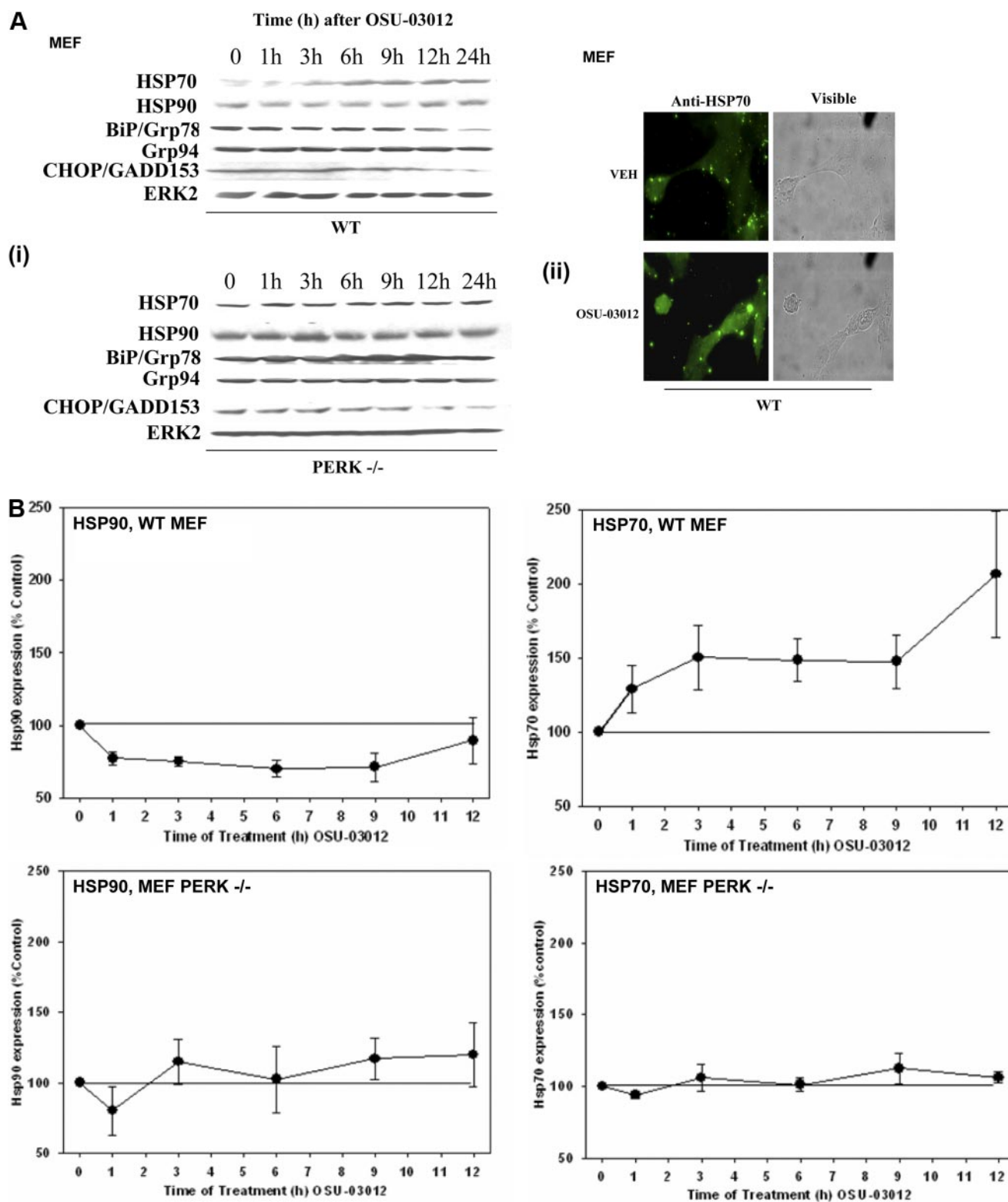
Fig. 5. OSU-03012 enhances HSP70 expression and suppresses Grp78/BiP levels in a PERK-dependent fashion. A, i, SV40-transformed WT and PERK$^{-/-}$ MEFs were cultured as described under *Materials and Methods*. Twenty-four hours after plating, cells were treated with DMSO vehicle or with OSU-03012 (OSU, 1 μM). Cells were isolated at the indicated time points and lysed. Cell lysates were subjected to SDS-PAGE and immunoblotting to determine the expression of HSP70, HSP90, BiP/Grp78, Grp94, CHOP/GADD153, and ERK2 ($n = 5$–7). ii, SV40-transformed WT were cultured as described under *Materials and Methods* on coated glass chamber slides. Twenty-four hours after plating, cells were treated with DMSO vehicle or with OSU-03012 (OSU, 1 μM). Cells were fixed 6 h after OSU-03012 treatment and stained with an anti-HSP70 antibody followed by a secondary antibody linked to FITC. Cells were visualized under fluorescent and visible light. A representative field is shown ($n = 2$ independent studies). B, the relative expression of HSP70 and HSP90 in OSU-03012-treated WT and PERK$^{-/-}$ MEFs from the time course analyses in A was calculated from the digital images in A and presented graphically ($\pm$ S.E.M., $n = 5$–7).
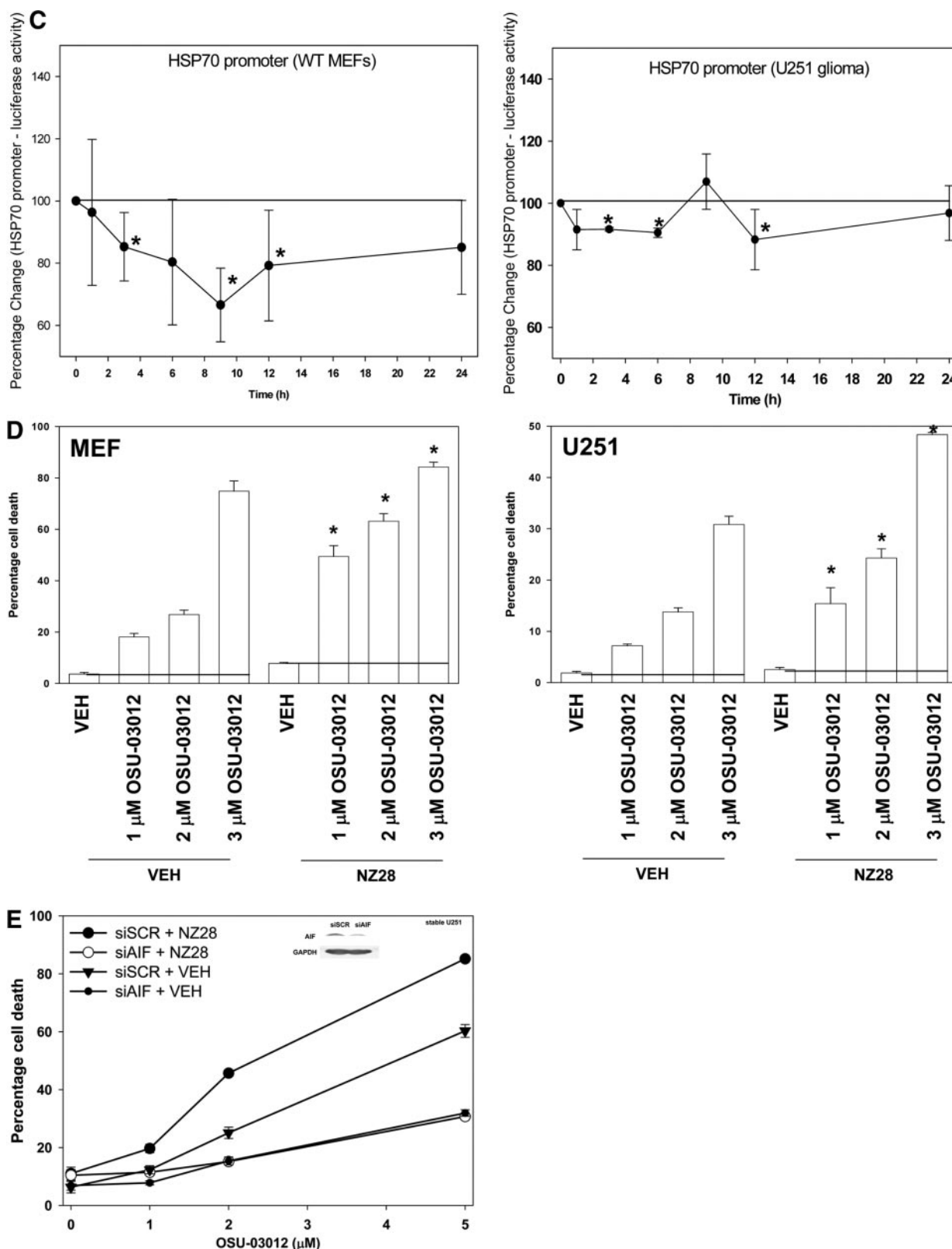
C, WT MEFs and U251 cells were plated and 12 h later transfected with a plasmid containing the full-length human HSP70 promoter coupled to the production of luciferase. Twenty-four hours after transfection, cells were treated with OSU-03012 (1 μM). The activity of the promoter was determined by luciferase activity in portions of cell lysate isolated at the indicated times. Data are a representative study in sextuplicate from three separate experiments ($\pm$ S.E.M.). D, twenty-four hours after plating, U251 cells and fibroblasts were treated with vehicle (VEH, DMSO) or with the HSP70 inhibitor NZ28 (1 μM) as indicated, followed 30 min later by vehicle (VEH, DMSO) or OSU-03012 (1–3 μM) as indicated. Cells were isolated 48 h after drug treatment by trypsinization. Cell viability was determined using a trypan blue exclusion assay in triplicate, and a representative experiment $\pm$ S.E.M. is shown from multiple experiments ($n = 3$). E, U251 cells were stably transfected with either a scrambled siRNA (siSCR) or an siRNA to knockdown expression of AIF (siAIF) (see also Fig. 1). Twenty-four hours after plating, cells were treated with vehicle (VEH, DMSO) or with NZ28 (1 μM) followed 30 min later by vehicle (VEH, DMSO) or OSU-03012 (OSU, 1 μM, 2 μM, 5 μM). Cells were isolated by trypsinization 48 h after drug treatments. Cell viability was determined using a trypan blue exclusion assay in triplicate $\pm$ S.E.M. Data are from a representative experiment ($n = 3$).
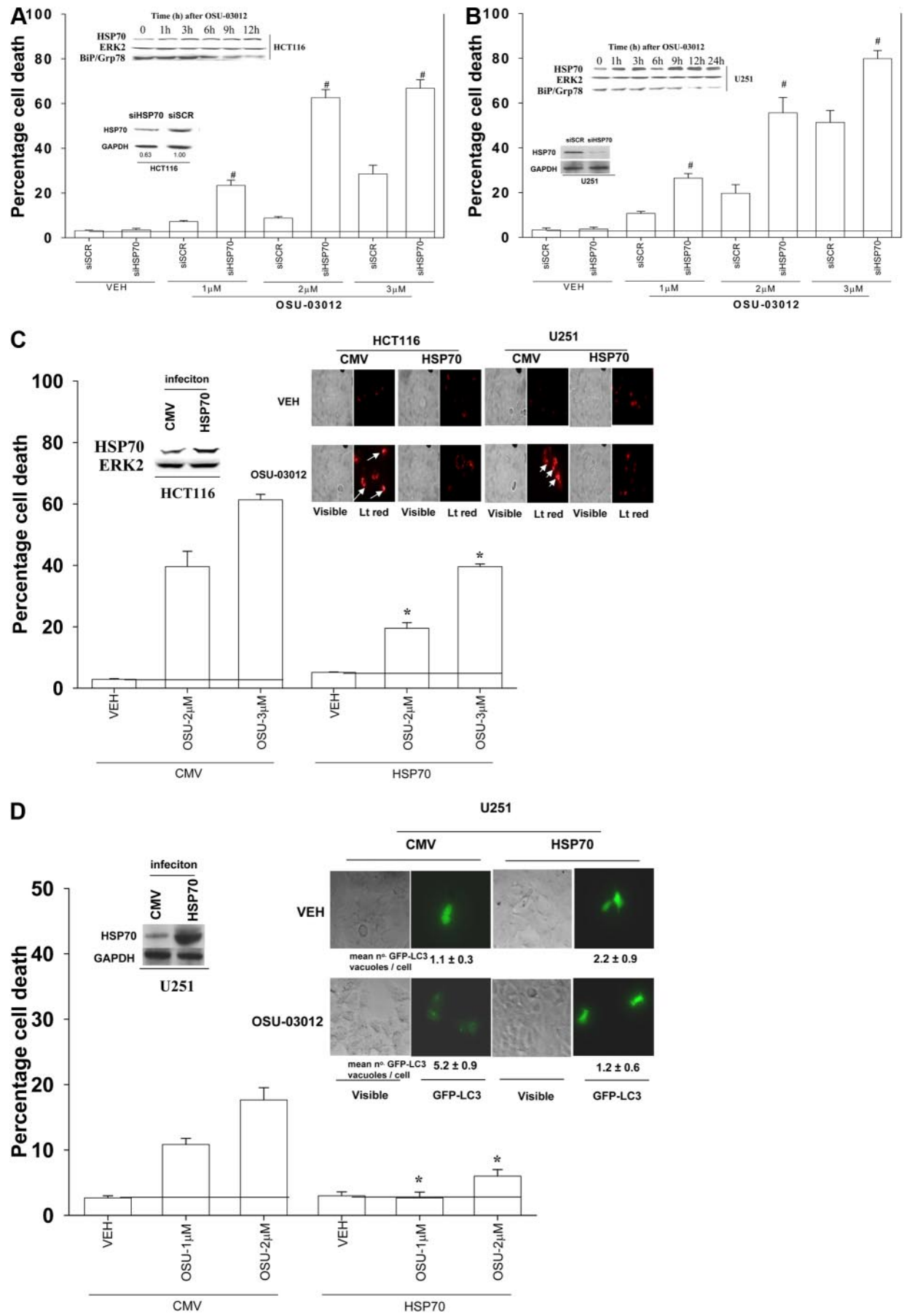
Grp78/BiP, a PERK binding protein, whose expression declined after OSU-03012 treatment, was noted to be protective against OSU-03012 toxicity (data not shown) (Lee, 2005). Overexpression of HSP70 suppressed the GFP-LC3 vacuolization response of OSU-03012–treated U251 cells as judged microscopically (Fig. 6D, inset). Thus, OSU-03012 causes cell death in a PERK-dependent fashion and increases expression of a protective protein, HSP70, in a PERK-dependent fashion, providing support for the contention that OSU-03012–induced PERK signaling promotes both cell survival and cell death processes.

In prior studies (Yacoub et al., 2006), we noted that inhibition of both the ERK1/2 and PI3K pathways enhanced OSU-03012 toxicity. A drug that could potentially mediate simultaneous inhibition of ERK1/2 and PI3K signaling is the geldanamycin 17AAG; however, geldanamycins also increase expression of HSP70, which could act to protect cells from OSU-03012 toxicity (Ravagnan et al., 2001; Nylandsted et al., 2004; Demidenko et al., 2006). Simultaneous exposure of transformed wild-type MEFs to 17AAG and OSU-03012 resulted in a greater than additive increase in cell killing (Fig. 7A). This effect was abolished in PERK$^{-/-}$ cells. In wild-type MEFs, 17AAG modestly increased the expression of HSP70 whereas in PERK$^{-/-}$ cells, 17AAG-induced HSP70 levels were very much greater (Fig. 7A, inset panel). Identical data were obtained in U251 glioma cells when dominant-negative PERK was expressed (Fig. 7B). These findings provide support for the contention that PERK signaling acts to suppress the induction of HSP70 expression after geldanamycin exposure and further emphasizes the protective role of HSP70 in maintaining viability.

Discussion

Previous studies have demonstrated that the novel celecoxib derivative OSU-03012, at concentrations an order of magnitude below those stably achievable in mouse plasma, and that are without observable normal tissue toxicity, killed hematopoietic, glioblastoma, lung, and colon cancer cells in vitro. In these studies, OSU-03012 toxicity was variously linked to inhibition of PDK-1 and to the induction of a form of ER stress signaling with activation of a cell death/cathepsin B-AIF pathway (Tseng et al., 2005, 2006; Yacoub et al., 2006; To et al., 2007). The present studies were initiated to further elucidate the molecular mechanisms by which OSU-03012 kills transformed cells in vitro.

OSU-03012 promoted a dose-dependent induction of transformed cell killing that was significantly reduced in U251 cells in which AIF expression was stably suppressed. Genetic deletion of cathepsin B suppressed OSU-03012–induced cleavage of BID, AIF release into the cytosol, and fibroblast cell killing. Loss of PERK function suppressed OSU-03012–induced activation of cathepsin B. OSU-03012 also promoted a PERK-dependent processing of pro-caspase 4, and knockdown of caspase 4 expression protected cells against OSU-03012 toxicity; cathepsin B activation was dependent upon caspase 4 in glioma cells. Together, these findings provide additional support to those previously reported by our laboratory and provide support for the argument that OSU-03012 causes activation of multiple pro-apoptotic proteases downstream of PERK, but independently of eIF2α and CHOP, to cause cell death (Yacoub et al., 2006).

OSU-03012 treatment caused a rapid ~3- to 6-h PERK-dependent induction of intracellular vesicles in human cancer cells and in rodent fibroblasts. The vacuolization effects included the appearance of low pH vesicles that stained for Lysotracker Red and vesicles that were associated with a transfected GFP-tagged LC3 protein. OSU-03012 increased the expression of ATG5 and Beclin 1 and promoted cleavage of endogenous LC3 protein in a PERK-dependent fashion. Knockdown of either ATG5 or Beclin 1 expression signifi-

Fig. 6. Modulation of HSP70 expression changes OSU-03012 lethality. A, HCT116 cells were cultured as described under *Materials and Methods* and, 12 h after plating, transfected with either a scrambled siRNA (siSCR) or an siRNA to suppress expression of HSP70 (siHSP70). Twenty-four hours after transfection, cells were treated with vehicle (VEH, DMSO) or with OSU-03012 (OSU, 0–3 μM). Cells were isolated by trypsinization 24 h after drug treatments. Cell viability was determined using a trypan blue exclusion assay in triplicate. Data are from a representative experiment ($n = 3$). (#, $p < 0.05$ greater than corresponding value in the siSCR cells). Inset, blots, bottom, HCT116 cells were lysed before OSU-03012 addition and the expression of HSP70 determined by immunoblotting. Top, HCT116 cells were treated with OSU-03012 (1 mM), cells isolated at the indicated time points, and the expression of HSP70, BiP/Grp78, and ERK2 determined by immunoblotting. B, U251 cells were cultured as described under *Materials and Methods* and 12 h after plating transfected with either a scrambled siRNA (siSCR) or an siRNA to suppress expression of HSP70 (siHSP70). Twenty-four hours after transfection, cells were treated with vehicle (VEH, DMSO) or with OSU-03012 (OSU, 0–3 μM). Cells were isolated by trypsinization 24 h after drug treatments. Cell viability was determined using a trypan blue exclusion assay in triplicate. Data are from a representative experiment ($n = 3$). (#, $p < 0.05$ greater than corresponding value in the siSCR cells). Inset, blotting, bottom, U251 cells were lysed before OSU-03012 addition and the expression of HSP70 determined by immunoblotting. Top, U251 cells were treated with OSU-03012 (1 mM), cells isolated at the indicated time points, and the expression of HSP70, BiP/Grp78, and ERK2 determined by immunoblotting. C, HCT116 cells were cultured as described under *Materials and Methods* and, 12 h after plating, were infected with either an empty vector control recombinant adenovirus (CMV) or an adenovirus to express HSP70. Twenty-four hours after infection, cells were treated with vehicle (VEH, DMSO) or with OSU-03012 (OSU, 2 μM, 3 μM). Cells were isolated by trypsinization 24 h after drug treatments. Cell viability was determined using a trypan blue exclusion assay in triplicate. Data are from a representative experiment ($n = 3$). *, $p < 0.05$ less than corresponding value in the CMV-infected cells. Inset, microscopy, U251 and HCT116 cells were plated in four-chamber glass slides and, 12 h after plating, were infected with either a control recombinant adenovirus (CMV) or a recombinant adenovirus to express HSP70. Twenty-four hours after infection, cells were treated with vehicle (DMSO) or with OSU-03012 (1 μM). Cells were fixed 6 h after drug exposure and stained with Lysotracker Red (Lt) dye. Cells were visualized at 40× using an Axiovert 200 fluorescent microscope under fluorescent light and visual light. Data shown is a representative field from one experiment ($n = 3$). White arrows denote areas of intense staining, indicative of vacuolization. Inset, blot, HCT116 cells were cultured as described under *Materials and Methods*. Twenty-four hours after infection, cells were treated with DMSO vehicle or with OSU-03012 (OSU, 1 μM). Cells were isolated at the indicated time points and lysed. Cells lysates were subjected to SDS PAGE and immunoblotting to determine the expression of HSP70, BiP/Grp78, and ERK2 ($n = 3$). D, U251 cells were cultured as described under *Materials and Methods*, and 12 h after plating infected with either an empty vector control recombinant adenovirus (CMV) or an adenovirus to express HSP70. Twenty-four hours after infection, cells were treated with vehicle (VEH, DMSO) or with OSU-03012 (OSU, 1 μM, 2 μM). Cells were isolated by trypsinization 24 h after drug treatments. Cell viability was determined using a trypan blue exclusion assay in triplicate. Data are from a representative experiment ($n = 3$). (*, $p < 0.05$ less than corresponding value in the CMV infected cells). Inset, microscopy, U251 cells were plated in four-chamber glass slides and, 12 h after plating, infected with either a control recombinant adenovirus (CMV) or a recombinant adenovirus to express HSP70. Twenty-four hours after infection, cells were transfected with a plasmid to express GFP-LC3. Twenty-four hours after transfection, cells were treated with vehicle (VEH, DMSO) or with OSU-03012 (1 μM). The appearance of punctate GFP-LC3 vacuoles was examined 6 h after drug exposure ($n = 2$). Inset, blotting, U251 cells were cultured as described under *Materials and Methods*. Twenty-four hours after infection, cells were lysed and were subjected to SDS-PAGE and immunoblotting to determine the expression of HSP70 and ERK2 ($n = 3$).

cantly reduced the PERK-dependent induction of vesicles that were associated with a transfected GFP-tagged LC3 protein. These findings, together with our prior work, provide strong support for the contention that OSU-03012 exposure causes an early autophagic response in transformed cell types that precedes the apparent AIF release into the cytosol or morphological (i.e., trypan blue-positive) manifestation of cell death (Yacoub et al., 2006).

Our prior findings with OSU-03012 were consistent with the hypothesis that OSU-03012 promotes lysosomal dysfunction and cathepsin protease translocation into the cytosol, which catalyzes BID cleavage that in turn promotes AIF release into the cytosol (Yacoub et al., 2006). In the present studies, we found that loss of PERK function blocked the

vacuolization of low pH vesicles, as well as those containing LC3, and the release of cathepsin B and AIF into the cytosol. Loss of cathepsin B function also suppressed low pH vesicle vacuolization, which provides evidence that the physical manifestation of the low pH vesicles was a secondary response after cathepsin B activation. In contrast, loss of cathepsin B function did not alter the induction of LC3-containing vacuoles, providing evidence that OSU-03012 induced true autophagic vesicles before causing either cathepsin B activation or the induction of low pH vesicle vacuolization. It has been observed by others that during an autophagic response, LC3 concentration into vacuoles increases at earlier than the low pH vacuolization effects observed using Lysotracker Red dye. The first step in autophagy has been shown
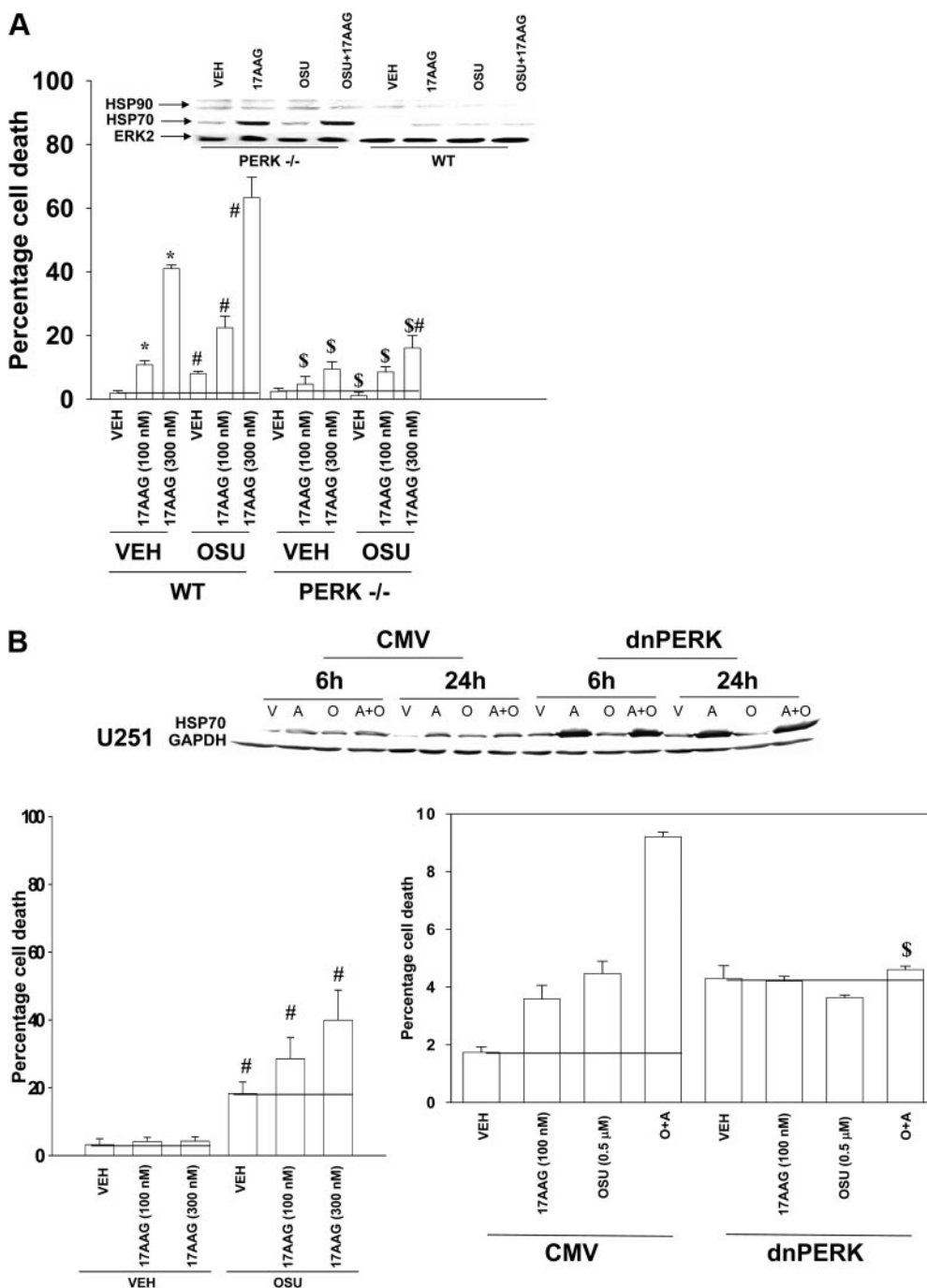

Fig. 7. Modulation of HSP70 expression changes OSU-03012 lethality. A, SV40-transformed WT and PERK$^{-/-}$ MEFs were cultured as described under *Materials and Methods*. Cells, 24 h after plating were treated with DMSO vehicle or with OSU-03012 (OSU, 1 μM) and or 17AAG (100 nM; 300 nM). Cells were isolated 24 h after drug exposure and cell viability was determined using a trypan blue exclusion assay in triplicate. Data are from a representative experiment ($n = 3$) (#, $p < 0.05$ greater than cells lacking OSU-03012 treatment; \$, $p < 0.05$ less than corresponding value in WT MEF cell. Inset, blotting, cells were lysed 12 h after OSU-03012 addition and the expression of ERK2, HSP70, and HSP90 determined by immunoblotting. B, U251 cells were cultured as described under *Materials and Methods* and 12 h after plating transfected with either an empty vector control plasmid (CMV) or a plasmid to express dominant negative PERK (dnPERK). Twenty-four hours after transfection, cells were treated with vehicle (VEH, DMSO) or with OSU-03012 (OSU, 0.5–1 μM) and/or 17AAG (100 nM, 300 nM). Cells were isolated by trypsinization 24 h after drug treatments. Cell viability was determined using a trypan blue exclusion assay in triplicate. Data are from a representative experiment ($n = 3$). (#, $p < 0.05$ greater than corresponding value in the CMV cells). Inset, blotting, U251 cells were lysed 6 h and 24 h after OSU-03012 (1 μM) and/or 17AAG (100 nM) addition and the expression of HSP70 and GAPDH determined by immunoblotting.

to be the envelopment of an organelle by the isolating membrane (Levine and Yuan, 2005; Yang et al., 2005; Shibata et al., 2006; Yousefi et al., 2006). This compartment is called an autophagosome, which is marked by the appearance of LC3 (Levine and Yuan, 2005; Yang et al., 2005; Shibata et al., 2006; Yousefi et al., 2006). The autophagosomes are then enveloped by the lysosomal compartment, forming autolysosomes, which are, in the case of our present studies, probably detected by the acidic vacuole stain Lysotracker Red. Thus, collectively, these data demonstrate that OSU-03012 causes a form of ER stress response that leads to activation of a PERK and lysosomal vacuolization-dependent cathepsin B/BID/AIF-dependent cell death pathway.

Celecoxib-induced apoptosis has been argued to be ER stress-dependent, the loss of GADD153 (CHOP) function preventing cell killing (Tsutsumi et al., 2004, 2006). In this model, basically, celecoxib-induced apoptosis would be impeded in cells lacking PERK expression, which is the opposite of our findings with OSU-03012 treatment, wherein transformed fibroblasts were more resistant to drug toxicity when PERK was not expressed. Indeed, parallel studies in wild-type and PERK$^{-/-}$ cells using OSU-03012 and thapsigargin demonstrate diametrically opposite effects in drug sensitivity. Knockdown of CHOP expression modestly reduced OSU-03012 toxicity in transformed MEFs but had no effect on survival in HCT116 or U251 cells (M. A. Park and P. Dent, unpublished observations). OSU-03012 decreased Grp78/BiP expression and had no affect on CHOP expression, whereas in a classic ER stress response, the expression of these proteins would be expected to rise (Ron, 2002; Rutkowski and Kaufman, 2004). We noted recently that the novel drug sorafenib, which has multiple intracellular targets, caused an ER stress response that also correlated with a reduction in the expression of Grp78/BiP, suggesting that the response pattern we observed with OSU-03012 may be a characteristic of drugs that inhibit both "signaling pathways" and that also cause ER stress responses (Rahmani et al., 2007). Of additional note with respect to the actions of OSU-03012, some novel agents [e.g., the proteasome inhibitor bortezomib (Velcade)] have been shown to kill tumor cells via increased expression of ER stress markers such as CHOP while inhibiting PERK activity and the phosphorylation of eiF2α (Nawrocki et al., 2005).

It has been noted in many studies that tumor cells, when exposed to moderately toxic concentrations of therapeutic agents, exhibit compensatory survival responses by activating survival signaling pathways or by increasing the expression of certain proteins that maintain cell viability (reviewed in Grant and Dent, 2004). Classic ER stress signaling has also been noted to promote either a toxic response (e.g., elevated CHOP expression) or a protective response (e.g., enhanced BiP/Grp78 expression) based on the duration or intensity of the stress signal (Rahmani et al., 2007). OSU-03012 treatment of transformed human and rodent cells initially increased expression of HSP70 in parallel to the formation of autophagic vacuoles, which are both putatively protective effects, in a PERK-dependent fashion. However, OSU-03012 treatment of cells then subsequently caused a decrease in HSP90 and BiP/Grp78 expression in parallel to the release of cathepsin B and AIF into the cytosol, all of which are putatively toxic effects, and these effects also occurred in a PERK-dependent fashion. In HCT116 and U251

cells, overexpression of HSP70 suppressed, and knockdown of HSP70 levels enhanced, OSU-03012 toxicity. Overexpression of HSP70 blocked acidic endosome vacuolization, in general agreement with the findings of others (e.g., Nylandsted et al., 2004). Collectively, these findings support the hypothesis that OSU-03012 causes a form of ER stress that induces a protective PERK-dependent response involving elevated expression of HSP70 and autophagic vesicle formation. This ultimately degenerates, however, presumably because of prolonged PERK signaling, into a cytotoxic response with the formation of low pH acidic endosomes and the release of cathepsin B and AIF into the cytosol, which causes a non-apoptotic form of cell death.

Increased expression of HSP70 has been shown by several groups to stabilize endosomes, to suppress the apoptotic activity of AIF, and collectively to promote cell survival (Mosser et al., 2000; Ravagnan et al., 2001; Gurbuxani et al., 2003; Nylandsted et al., 2004; Demidenko et al., 2006; Mambula and Calderwood, 2006). In our analyses, we demonstrated that overexpression of HSP70 blocked the formation of GFP-LC3 vacuoles and low pH acidic endosomes after OSU-03012 exposure, demonstrating that one site at which HSP70 acted to promote survival after OSU-03012 treatment was at the earliest stages of ER stress signaling. However, our data in U251 cells, in which we modified HSP70 function using the pharmacologic agent NZ28, also suggested that HSP70 could act downstream in the cell death pathway at the level of AIF. Because OSU-03012 was competent to overcome the protective effects of compensatory increases in HSP70 expression, it is tempting to speculate whether this compound might act as a general suppressive agent of "protective" HSP70 function at multiple sites.

Recent studies in human myeloma cells using concentrations of OSU-03012 approximately 1 order of magnitude higher than our studies reported that cell killing was inhibited by neither caspase nor cathepsin inhibitors (Zhang et al., 2007). These studies also noted that BID cleavage occurred in response to OSU-03012 exposure. Because both caspase 2 and caspase 4 have been shown to cleave BID independently of cathepsin protease action, it is possible that some cells may primarily use caspases 2 and 4, which are generally insensitive to "pan" caspase inhibitors such as zVAD, to process BID into its active form after OSU-03012 exposure rather than cathepsin proteases (Ekert et al., 1999; Hitomi et al., 2004; Yeung et al., 2006).

In conclusion, the regulation of transformed cell survival after treatment of cells with low doses of OSU-03012 seems to be complicated and multifactorial. OSU-03012 activates PERK, which, 1) through a yet-to-be-identified eiF2α-independent mechanism, stimulates autophagic vacuolization, which plays a role in the activation of cathepsin proteases; 2) caspase 4- and cathepsin-dependent complete vacuolization of LC3 containing vesicles into Lysotracker Red staining low pH vesicles and a subsequent enhancement in cell killing via BID cleavage (Stoka et al., 2001; Lamparska-Przybysz et al., 2005; Yeung et al., 2006); and 3) promotes increased expression of HSP70, which acts to suppress cell killing potentially by blocking vacuolization processes and the lethal actions of AIF. Further studies beyond the scope of this article will be required to fully define how OSU-03012 regulates PERK, caspase 4, and AIF function.

References

Carón RW, Yacoub A, Li M, Zhu X, Mitchell C, Hong Y, Hawkins W, Sasazuki T, Shirasawa S, Kozikowski AP, Dennis PA, Hagan MP, Grant S, and Dent P (2005) Activated forms of H-RAS and K-RAS differentially regulate membrane association of PI3K, PDK-1, and AKT and the effect of therapeutic kinase inhibitors on cell survival. *Mol Cancer Ther* **4:**257–270.

Cui W, Yu CH, and Hu KQ (2005) In vitro and in vivo effects and mechanisms of celecoxib-induced growth inhibition of human hepatocellular carcinoma cells. *Clin Cancer Res* **11:**8213–8221.

Demidenko ZN, Vivo C, Halicka HD, Li CJ, Bhalla K, Broude EV, and Blagosklonny MV (2006) Pharmacological induction of Hsp70 protects apoptosis-prone cells from doxorubicin: comparison with caspase inhibitor- and cycle-arrest-mediated cytoprotection. *Cell Death Differ* **13:**1434–1441.

Dent P, Yacoub A, Fisher PB, Hagan MP, and Grant S (2003) MAPK pathways in radiation responses. *Oncogene* **22:**5885–5896.

Dunn WA (1994) Autophagy and related mechanisms of lysosome-mediated protein degradation. *Trends Cell Biol* **4:**139–143.

Ekert PG, Silke J, and Vaux DL (1999) Caspase inhibitors. *Cell Death Differ* **6:**1081–1086.

Fehrenbacher N, Gyrd-Hansen M, Poulsen B, Felbor U, Kallunki T, Boes M Weber E, Leist M, and Jäättelä M (2004) Sensitization to the lysosomal cell death pathway upon immortalization and transformation. *Cancer Res* **64:**5301–5310.

Grant S and Dent P (2004) Kinase inhibitors and cytotoxic drug resistance. *Clin Cancer Res* **10:**2205–2207.

Gurbuxani S, Schmitt E, Cande C, Parcellier A, Hammann A, Daugas E Kouranti I, Spahr C, Pance A, Kroemer G, and Garrido C (2003) Heat shock protein 70 binding inhibits the nuclear import of apoptosis-inducing factor. *Oncogene* **22:**6669–6678.

Hart LS, Ornelles D, Koumenis C (2007) The adenoviral E4orf6 protein induces atypical apoptosis in response to DNA damage. *J Biol Chem* **282:**6061–6067.

Hawkey CJ and Fortun PJ (2005) Cyclooxygenase-2 inhibitors. *Curr Opin Gastroenterol* **21:**660–664.

Hitomi J, Katayama T, Eguchi Y, Kudo T, Taniguchi M, Koyama Y, Manabe T, Yamagishi S, Bando Y, Imaizumi K, et al. (2004) Involvement of caspase-4 in endoplasmic reticulum stress-induced apoptosis and Aβ-induced cell death. *J Cell Biol* **165:**347–356.

Johnson AJ, Smith LL, Zhu J, Heerema NA, Jefferson S, Mone A, Grever M, Chen CS, and Byrd JC (2005) A novel celecoxib derivative, OSU03012, induces cytotoxicity in primary CLL cells and transformed B-cell lymphoma cell line via a caspase- and Bcl-2-independent mechanism. *Blood* **105:**2504–2509.

Kabeya Y, Mizushima N, Ueno T, Yamamoto A, Kirisako T, Noda T, Kominami E, Ohsumi Y, and Yoshimori T (2000) LC3, a mammalian homologue of yeast Apg8p, is localized in autophagosome membranes after processing. *EMBO J* **19:**5720–5728.

Kang SG, Kim JS, Park K, Kim JS, Groves MD, and Nam DH (2006) Combination celecoxib and temozolomide in C6 rat glioma orthotopic model. Oncol Rep 15:7–13.

Kashfi K and Rigas B (2005) Is COX-2 a 'collateral' target in cancer prevention? *Biochem Soc Trans* **33:**724–727.

Kiefer W and Dannhardt G (2004) Novel insights and therapeutical applications in the field of inhibitors of COX-2. *Curr Med Chem* **11:**3147–3161.

Klenke FM, Gebhard MM, Ewerbeck V, Abdollahi A, Huber PE, and Sckell A (2006) The selective Cox-2 inhibitor celecoxib suppresses angiogenesis and growth of secondary bone tumors: an intravital microscopy study in mice. *BMC Cancer* **6:**9.

Koehne CH and Dubois RN (2004) COX-2 inhibition and colorectal cancer. *Semin Oncol* **31:**12–21.

Kulp SK, Yang YT, Hung CC, Chen LF, Lai JP, Tseng PH, Fowble JW, Ward PJ, and Chen CS (2004) 3-phosphoinositide-dependent protein kinase-1/Akt signaling represents a major cyclooxygenase-2-independent target for celecoxib in prostate cancer cells. *Cancer Res* **64:**1444–1451.

Lakka SS, Gondi CS, and Rao JS (2005) Proteases and glioma angiogenesis. *Brain Pathol* **15:**327–341.

Lamparska-Przybysz M, Gajkowska B, and Motyl T (2005) Cathepsins and BID are involved in the molecular switch between apoptosis and autophagy in breast cancer MCF-7 cells exposed to camptothecin. *J Physiol Pharmacol* **56:**159–179.

Lee AS (2005) The ER chaperone and signaling regulator GRP78/BiP as a monitor of endoplasmic reticulum stress. *Methods* **35:**373–381.

Levine B and Yuan J (2005) Autophagy in cell death: an innocent convict? *J Clin Invest* **115:**2679–2688.

Mambula SS and Calderwood SK (2006) Heat shock protein 70 is secreted from tumor cells by a nonclassical pathway involving lysosomal endosomes. *J Immunol* **177:**7849–7857.

McKinstry R, Qiao L, Yacoub A, Dai Y, Decker R, Holt S, Hagan MP, Grant S, Dent P (2002) Inhibitors of MEK1/2 interact with UCN-01 to induce apoptosis and reduce colony formation in mammary and prostate carcinoma cells. *Cancer Biol Ther* **1:**243–253.

Mosser DD, Caron AW, Bourget L, Meriin AB, Sherman MY, Morimoto RI, and Massie B (2000) The chaperone function of hsp70 is required for protection against stress-induced apoptosis. *Mol Cell Biol* **20:**7146–7159.

Narayanan BA, Narayanan NK, Pttman B, and Reddy BS (2006) Adenocarcina of the mouse prostate growth inhibition by celecoxib: downregulation of transcription factors involved in COX-2 inhibition. *Prostate* **66:**257–265.

Nawrocki ST, Carew JS, Dunner K Jr., Boise LH, Chiao PJ, Huang P Abbruzzese JL, and McConkey DJ (2005) Bortezomib inhibits PKR-like endoplasmic reticulum (ER) kinase and Induces apoptosis via ER stress in human pancreatic cancer cells. *Cancer Res* **65:**11510–11519.

Nylandsted J, Gyrd-Hansen M, Danielewicz A, Fehrenbacher N, Lademann U, Hoyer-Hansen M Weber E, Multhoff G, Rohde M, and Jäättelä M (2004) Heat shock protein 70 promotes cell survival by inhibiting lysosomal membrane permeabilization. *J Exp Med* **200:**425–435.

Patel MI, Subbaramaiah K, Du B, Chang M, Newman RA, Cordon-Cardo C Thaler HT, Dannenberg AJ (2005) Celecoxib inhibits prostate cancer growth: evidence of a cyclooxygenase-2-independent mechanism. *Clin Cancer Res* **11:**1999–2007.

Rahmani M, Davis EM, Crabtree TR, Habibi JR, Nguyen TK, Dent P, and Grant S (2007) The kinase inhibitor sorafenib induces cell death through a process involving induction of ER stress. *Mol Cell Biol* **27:**5499–5513.

Ravagnan L, Gurbuxani S, Susin SA, Maisse C, Daugas E Zamzami N, Mak T, Jäättelä M, Penninger JM, Garrido C, and Kroemer G (2001) Heat-shock protein 70 antagonizes apoptosis- inducing factor. *Nat Cell Biol* **3:**839–843.

Ron D (2002) Translational control in the endoplasmic reticulum stress response. *J Clin Invest* **110:**1383–1398.

Rutkowski DT and Kaufman RJ (2004) A trip to the ER: coping with stress. *Trends Cell Biol* **14:**20–28.

Seglen PO and Bohley P (1992) Autophagy and other vacuolar protein degradation mechanisms. *Experientia* **48:**158–172.

Shibata M, Lu T, Furuya T, Degterev A, Mizushima N, Yoshimori T MacDonald M, Yankner B, and Yuan J (2006) Regulation of intracellular accumulation of mutant Huntingtin by Beclin 1. *J Biol Chem* **281:**14474–14485.

Stoka V, Turk B, Schendel SL, Kim TH, Cirman T, Snipas SJ, Ellerby LM, Bredesen D, Freeze H, Abrahamson M, et al. (2001) Lysosomal protease pathways to apoptosis. Cleavage of bid, not pro-caspases, is the most likely route. *J Biol Chem* **276:**3149–3157.

To K, Zhao Y, Jiang H, Hu K, Wang M, Wu J, Lee C, Yokom DW, Stratford AL, Klinge U, et al. (2007) The phosphoinositide-dependent kinase-1 inhibitor 2-amino-*N*-[4-[5-(2-phenanthrenyl)-3-(trifluoromethyl)-1*H*-pyrazol-1-yl]phenyl]-acetamide (OSU-03012) prevents Y-box binding protein-1 from inducing epidermal growth factor receptor. *Mol Pharmacol* **72:**641–652.

Tseng PH, Lin HP, Zhu J, Chen KF, Hade EM, Young DC, Byrd JC, Grever M, Johnson K, Druker BJ, et al. (2005) Synergistic interactions between imatinib mesylate and the novel phosphoinositide-dependent kinase-1 inhibitor OSU-03012 in overcoming imatinib mesylate resistance. *Blood* **105:**4021–4027.

Tseng PH, Wang YC, Weng SC, Weng JR, Chen CS, Brueggemeier RW, Shapiro CL, Chen CY, Dunn SE, Pollak M, et al. (2006) Overcoming trastuzumab resistance in HER2-overexpressing breast cancer cells by using a novel celecoxib-derived phosphoinositide-dependent kinase-1 inhibitor. *Mol Pharmacol* **70:**1534–1541.

Tsutsumi S, Gotoh T, Tomisato W, Mimo S, Hoshino T, Hwang HJ, Takenaka H, Tsuchiya T, Mori M, and Mizushima T (2004) Endoplasmic reticulum stress response is involved in nonsteroidal anti-inflammatory drug-induced apoptosis. *Cell Death Differ* **11:**1009–1016.

Tsutsumi S, Namba T, Tanaka KI, Arai Y, Ishihara T, Aburaya M Mima S, Hoshino T, Mizushima T (2006) Celecoxib upregulates endoplasmic reticulum chaperones that inhibit celecoxib-induced apoptosis in human gastric cells. *Oncogene* **25:**1018–1029.

Valerie K, Yacoub A, Hagan MP, Curiel DT, Fisher PB, Grant S, and Dent P (2007) Radiation-induced cell signaling: inside-out and outside-in. *Mol Cancer Ther* **6:**789–801.

Yacoub A, Mitchell C, Hong Y, Gopalkrishnan RV, Su ZZ, Gupta P Sauane M, Lebedeva IV, Curiel DT, Mahasreshti PJ, Rosenfeld MR, et al. (2004) MDA-7 regulates cell growth and radiosensitivity in vitro of primary (non-established) human glioma cells. *Cancer Biol Ther* **3:**739–751.

Yacoub A, Park MA, Hanna D, Hong Y, Mitchell C, Pandya AP Harada H, Powis G, Chen CS, Koumenis C, Grant S, et al. (2006) OSU-03012 promotes caspase-independent but PERK-, cathepsin B-, BID-, and AIF-dependent killing of transformed cells. *Mol Pharmacol* **70:**589–603.

Yang YP, Liang ZQ, Gu ZL, and Qin ZH (2005) Molecular mechanism and regulation of autophagy. *Acta Pharmacol Sin* **26:**1421–1434.

Yeung BH, Huang DC, and Sinicrope FA (2006) PS-341 (Bortezomib) induces lysosomal cathepsin B release and a caspase-2-dependent mitochondrial permeabilization and apoptosis in human pancreatic cancer cells. *J Biol Chem* **281:**11923–11932.

Yousefi S, Perozzo R, Schmid I, Ziemecki A, Schaffner T, Scapozza L, Brunner T, and Simon HU (2006) Calpain-mediated cleavage of Atg5 switches autophagy to apoptosis. *Nat Cell Biol* **8:**1124–1132.

Zhang S, Suvannasankha A, Crean CD, White VL, Johnson A, Chen CS, and Farag SS (2007) OSU-03012, a novel celecoxib derivative, is cytotoxic to myeloma cells and acts through multiple mechanisms. *Clin Cancer Res* **13:**4750–4758.

Zhu J, Huang JW, Tseng PH, Yang YT, Fowble JW, Shiau CW, Shaw YJ, Kulp SK, and Chen CS (2004) From the cyclooxygenase-2 inhibitor celecoxib to a novel class of 3-phosphoinositide-dependent protein kinase-1 inhibitors. *Cancer Res* **64:**4309–4318.

Address correspondence to: Dr. Paul Dent, Department of Biochemistry, 401 College Street, Massey Cancer Center, Room 280a, Box 980035, Virginia Commonwealth University, Richmond, VA 23298-0035. E-mail: pdent@vcu.edu